Polyoxometalates REVIEW

Synergistic catalysis in POM@MOF and POM@COF composites: Emerging platforms for catalytic oxidation of sulfur-containing compounds

Yanhong Chen [1], Shenzhen Chang [2,3], and Junwei Zhao [2]

[1] *Key Laboratory of Electrochemical Energy Storage and Energy Conversion of Hainan Province, Key Laboratory of Electrochemical Energy Storage and Energy Conversion Materials of Haikou, School of Chemistry and Chemical Engineering, Hainan Normal University, Haikou 571158, China*

[2] *Henan Key Laboratory of Polyoxometalate Chemistry, College of Chemistry and Molecular Sciences, Henan University, Kaifeng, 475004, China*

[3] *Key Laboratory of Advanced Materials of Tropical Island Resources of Ministry of Education, School of Chemistry and Chemical Engineering, Hainan University, Haikou 570228, China*

Received: 22 May 2026; **Revised:** 19 June 2026; **Accepted:** 30 June 2026

Address correspondence to Shenzhen Chang, csz138250@hainanu.edu.cn; Junwei Zhao, zhaojunwei@henu.edu.cn

Cite This: *Polyoxometalates*, 2026, *5*, 9140146 https://doi.org/10.26599/POM.2026.9140146

ABSTRACT: The catalytic oxidation of sulfur-containing compounds constitutes a pivotal research frontier with broad implications across biomedicine, environmental remediation, and chemical defense. Polyoxometalates (POMs), well-defined anionic metal–oxygen clusters exhibiting tunable redox activity, high acidity and structural robustness, represent promising molecular catalytic units for selective sulfur oxidation. Yet their practical application is frequently hampered by, aggregation and limited recoverability under reaction conditions, particularly in polar media. Porous framework materials, notably metal–organic frameworks (MOFs) and covalent organic frameworks (COFs), offer structurally precise, modular scaffolds for the spatial confinement and stabilization of POMs. Host–guest composites engineered *via* encapsulation within framework cavities or channel walls not only suppress POM degradation and leaching but also synergistically enhance active-site accessibility, substrate diffusion and orientation, and interfacial charge-transfer kinetics. Existing reviews predominantly focus on single host systems or specific applications (e.g. only fuel oxidative desulfurization), failing to systematically encompass all three core research fields. This review comprehensively summarizes recent advances in POM@MOF and POM@COF composites in the fields of bioactive sulfide synthesis, fuel desulfurization and chemical warfare agent purification. The intrinsic correlations between host-guest interactions and catalytic performance, stability, as well as reaction mechanisms are discussed, and the future development directions in this field are prospected, aiming to facilitate the industrial application of related technologies.

KEYWORDS: polyoxometalates (POMs); metal–organic frameworks (MOFs); covalent organic frameworks (COFs); sulfide oxidation; heterogeneous catalysis; synergistic catalysis

1 Instructions

The oxidation reactions of sulfur-containing compounds represent a core research domain spanning biomedicine, environmental remediation, and public safety, where advancements in catalytic systems consistently remain at the cutting edge of green catalysis and organic synthesis [1-6]. In the life sciences, the selective oxidation of sulfides is not only crucial for constructing chiral sulfoxide drugs (such as proton pump inhibitors like omeprazole and antitumor drug candidates) but also intricately involved in the precise regulation of oxidative stress homeostasis in vivo [7-9]. In the environmental and safety sectors, oxidative desulfurization (ODS) of organic sulfur compounds in fuel is the core technological pathway for achieving ultra-low sulfur fuels and meeting stringent global environmental regulations [10, 11]. Meanwhile, the oxidative degradation of sulfur mustard (SM) and the purification of industrial sulfur-containing wastewater also put forward an urgent need for an efficient and stable oxidation catalytic system [4, 12]. The traditional oxidation processes for sulfur-containing compounds have long been hampered by an excessive reliance on stoichiometric high-valent metal oxidants and strong inorganic acids. Their inherent drawbacks in atom economy and the secondary environmental pollution caused by heavy-metal-containing waste streams have become a heavy shackle constraining industrial progress [13]. In alignment with the evolving trends of green chemistry, the development of efficient, green, and sustainable oxidation-catalysis systems represents not only an essential pathway to address issues of over-oxidation side reactions and secondary pollution, but also the key to advancing sulfur-containing compound transformation technologies toward sustainable development [14, 15].

Polyoxometalates (POMs), a well-defined class of anionic metal-oxygen clusters with a long history in inorganic chemistry, have undergone exactly two centuries of development up to now since Berzelius first reported phosphomolybdic acid in 1826 [16-18]. These nanoscale clusters, formed by the bridging of oxygen atoms between high-valence early transition metals (e.g., Mo, W, V, Nb, Ta, etc.), demonstrate a series of unique and tunable physicochemical properties [18-20]. These include rapid and reversible multielectron redox properties, strong Brønsted acidity and proton-conducting behavior, ultrahigh negative charge density, and abundant coordination sites. These exceptional characteristics have driven the research of POMs beyond traditional catalysis, rapidly expanding into interdisciplinary frontiers such as energy conversion and storage, biomedicine, supramolecular assembly, and functional hybrid materials [21-23]. To this day, catalysis remains the most active research domain in POM chemistry [24-28]. However, the inherent polar ionic character of pure POMs causes them to leach readily in polar solvents, making recovery difficult. Their extremely low specific surface area and tendency to aggregate also limit the effective exposure of active sites. Furthermore, the lack of spatial confinement effects in homogeneous systems hinders precise selective catalysis with complex substrates [29-32]. Therefore, how to employ efficient heterogenization immobilization strategies to overcome leaching and aggregation while introducing structural confinement effects, thereby achieving a leap forward in the catalytic performance of POMs, has become a critical scientific challenge that urgently needs to be addressed in this field.

The emergence of porous framework materials, especially the emerging metal-organic frameworks (MOFs) and covalent organic frameworks (COFs), has provided an ideal host platform for the heterogenization and immobilization of POMs [31, 33-37]. Host-guest composite catalytic systems constructed through strategies such as pore confinement, electrostatic interactions, and covalent grafting have achieved a leapfrog improvement in performance [38, 39]. Firstly, the physical confinement and chemical anchoring effects of the frameworks completely resolve the long-standing technical challenge of POMs solubility and difficult recovery, significantly enhancing the catalyst cycling stability [40, 41]. Secondly, the high specific surface area induces highly dispersed POMs, while the unique size-sieving effect of the pores endows the material with exceptional exposure rates of active sites and superior substrate selectivity [42, 43]. Most critically, the synergistic effects arising from electron transfer between the host and guest, combined with the microenvironmental enrichment within the pores, not only precisely modulate the redox potential of the POMs to boost their intrinsic activity but also optimize the kinetics of the entire catalytic cycle, that is, from adsorption and enrichment to activation and conversion and finally to product desorption [44-46]. Such composite materials, which integrate structural stability with functional synergy, have now become the research frontier in the field of green oxidation of sulfur-containing compounds [4, 6].

Although several related reviews have been reported, existing works predominantly focus on a single host material system or a single application scenario (e.g., solely targeting oxidative desulfurization of fuels) [3-6, 47-49], and have yet to systematically cover the three core application spheres spanning biomedicine (e.g., selective oxidation of bioactive sulfides), environmental remediation (e.g., ODS of fuels), and public safety (e.g., degradation of SM). Based on the aforementioned research background and existing gaps, this review focuses on the highly promising novel sulfur-oxidation catalytic system of porous framework encapsulated POMs, and systematically outlines milestone advances in three key directions of precise synthesis of bioactive sulfides, oxidative desulfurization and purification of fuels, and green decontamination of chemical warfare agents such as SM. Centered on two representative porous carriers, namely COFs and MOFs, the article provides an in-depth analysis of host-guest interfacial electronic interactions, spatial confinement effects, and synergistic catalytic mechanisms, thereby establishing a clear structure-catalytic performance relationship. Furthermore, it objectively summarizes unresolved common scientific challenges and engineering bottlenecks in the field, with a focused discussion on the degradation mechanisms affecting long-term cycling stability and pathways for low-cost, scalable production. Finally, in light of the converging trends among materials chemistry, catalysis science, and environmental engineering, this review proposes key research directions warranting future breakthroughs, offering systematic theoretical guidance and conceptual insights to facilitate the translation of next-generation efficient sulfur-oxidation catalytic technologies from the laboratory to practical applications.

2 Synthesis Overview

Encapsulation is one of the core strategies for constructing POM@porous framework composite materials [25]. This strategy utilizes multiple non-covalent weak interactions such as hydrogen bonds, van der Waals forces, anion-π interactions, host-guest recognition, hydrophobic interactions, and electrostatic attractions as collaborative driving forces to achieve the confined assembly and stable immobilization of POM clusters within the pores of the porous framework. Moreover, this structure does not require covalent modification of POM or the framework skeleton, has lower requirements for charge matching between the two, and has mild reaction conditions, which can maximize the retention of the intrinsic structure and activity of POM, while also taking into account the crystallinity and pore integrity of the framework material. It demonstrates unique advantages in the composite of framework systems and function-sensitive POMs.

2.1 Synthesis of POM@MOFs

MOFs combine the coordination diversity of metal nodes with the designable functionality of organic linkers. Their pore cavities provide abundant supramolecular interaction sites, offering diverse interfaces for the supramolecular encapsulation of POMs [50-53]. Depending on the assembly sequence and reaction pathway, the synthesis of

supramolecular POM@MOFs is mainly divided into two categories: the *in-situ* one-pot supramolecular assembly method and the post-synthetic host-guest impregnation method. These strategies not only realize the complementary advantages of two types of functional units, inorganic POM units and organic-inorganic MOF frameworks, but more importantly, it generates a synergistic catalytic effect that cannot be compared with a single component through the strong electronic interaction at the interface and the nanospace confinement effect [54-57]. Firstly, by regulating electron transfer between POMs and MOFs, the electronic structure and redox potential of active centers are effectively tuned, optimizing the adsorption energy of reactants and intermediates. Secondly, the porous MOF skeleton provides a confined space for catalytic reactions, which not only stabilizes highly reactive intermediates but also significantly enhances selectivity toward target products through size and shape selectivity. Thirdly, highly dispersed POM active sites cooperate with the conductive framework of MOFs to accelerate charge transfer during catalysis and lower the reaction energy barrier.

2.1.1. In-situ one-pot assembly method

The *in-situ* one-pot method involves simultaneously adding POM precursors, metal salts, and organic linkers into the reaction system. Under thermodynamically controlled hydrothermal/solvothermal conditions, the coordination assembly of the MOF framework and the encapsulation of POMs within the pores are completed synchronously. Unlike electrostatic *in-situ* synthesis, which relies on strong charge matching, the core driving force for supramolecular *in-situ* assembly stems from the synergistic effects of hydrogen bonding between the surface oxygen atoms of the POM and the functional groups of the MOF linkers, anion-π weak interactions between aromatic linkers and POM clusters, and solvation effects, rather than a single electrostatic attraction.

In this method, POMs can simultaneously act as supramolecular templates. Through weak interactions, they induce the directional nucleation and growth of MOF precursors around them, ultimately completely encapsulating the POMs within the framework pores, effectively preventing surface aggregation and leaching of POMs. By adjusting the pH, solvent polarity, and reactant ratios of the reaction system, the strength of supramolecular interactions can be precisely regulated, thereby controlling the loading amount and dispersion state of POMs. This strategy is suitable for MOF systems whose linkers contain hydrogen bond donor groups such as hydroxyl or amino groups, and for POM clusters with low charge density that are difficult to immobilize *via* strong electrostatic interactions. It enables efficient encapsulation without introducing additional charge modifications.

2.1.2 Post-synthetic host-guest impregnation assembly method

The post-synthetic impregnation method uses pre-synthesized and fully activated MOF crystals as the host. These are immersed in an aqueous or organic solvent dispersion of POMs. Relying on concentration gradients, POM molecules diffuse into the MOF channels, and are then adsorbed and fixed *via* multiple supramolecular interactions within the pores. Compared to the *in-situ* method, this approach features mild reaction conditions, requiring no high temperature or pressure throughout the process. It completely avoids interference of POMs with the MOF crystallization process, maximally preserving the intrinsic topology and pore parameters of the MOF.

To enhance supramolecular binding, MOFs with functionalized linkers are typically chosen as carriers. For example, UiO-series MOFs with linkers modified with amino or hydroxyl groups can form stable supramolecular interaction networks with terminal or bridging oxygen atoms of POMs *via* hydrogen bonding. MOFs containing aromatic fused-ring linkers can generate additional binding force with negatively charged POMs through anion-π interactions. Furthermore, controlling the diffusion rate of POMs *via* slow solution diffusion methods (e.g., liquid-liquid layering diffusion, vapor diffusion) enables uniform, stepwise adsorption of POMs within the channels, preventing pore blockage and surface aggregation. This method is particularly suitable for POM systems with poor thermal stability or structures prone to decomposition under hydrothermal conditions, and for constructing functional materials that require high framework crystallinity.

2.1 Synthesis of POM@COFs

COFs are crystalline porous polymers formed by the covalent linkage of organic monomers [58-60]. Composed entirely of light elements (such as C, H, O, N, B, etc.), their core advantages lie in their pre-designable structures and permanently open pores. COFs not only possess extremely high specific surface areas and exceedingly good physicochemical stability but can also incorporate specific functional units (such as redox-active centers or extended π-conjugated systems) to achieve atomic-level precision in regulating charge transfer and mass diffusion. Since their first report in 2005, COFs have demonstrated immense potential in cutting-edge fields such as environmental catalysis, water treatment, and selective oxidation [61, 62]. Moreover, the highly open pore structure of COFs makes them reliable molecular carriers, capable of efficiently capturing and immobilizing various functional guest molecules. For example, through spatial confinement effects or electrostatic assembly strategies, COFs can precisely anchor guest molecules like POMs [63], effectively suppressing the aggregation and leaching of active components, achieving performance breakthroughs in photoelectrocatalysis, environmental remediation (e.g. selective oxidation in complex aqueous environments), and energy conversion [33, 41]. This system integrates a long-range ordered crystalline network with an exceptionally stable aromatic skeleton. Leveraging host-guest synergy at the molecular level, it provides a broad platform for developing the next generation of highly efficient and stable composite catalytic materials. The synthesis of POM@COFs primarily employs the post-synthetic adsorption method, with the in-situ copolymerization encapsulation strategy serving as a supplementary approach.

2.2.1 Post-synthetic adsorption method

Post-synthetic adsorption is currently the mainstream

strategy for preparing supramolecular POM@COFs. Its synthetic procedure consists of two steps. First, the COF carriers with the desired pore size and functional groups is synthesized *via* solvothermal or interfacial polymerization; the activated COF is then immersed in a POM solution, and POM diffusion into the pores and supramolecular immobilization are achieved by standing or stirring.

The core driving force of this method stems from the synergy of two aspects: one is the anion-π interaction between the conjugated framework of the COF and the negatively charged POM clusters. This is the key supramolecular force for immobilizing POMs in electrically neutral COFs, and it plays a particularly significant role in electron-rich conjugated COF systems such as triazine-based or porphyrin-based COFs. The other is the multiple hydrogen-bonding network formed between functional groups on the pore walls (e.g., amino, hydroxyl, imine bonds) and the surface oxygen atoms of the POM, which further enhances the binding stability. By regulating the matching between the pore size of the COF and the POM cluster, combined with optimization of solution concentration, impregnation time, and temperature, monodisperse and uniform loading of POMs within the one-dimensional channels of the COF can be achieved while retaining the high crystallinity and ordered pore structure of the COF. This method avoids interference of POMs with the covalent polycondensation process of the COF and represents a reliable route to construct highly crystalline POM@COF composites.

2.2.2 In-situ copolymerization supramolecular encapsulation method

The in-situ copolymerization method directly introduces POM clusters into the polymerization system of the COF. During the covalent condensation of monomers to form the COF framework, supramolecular interactions (such as π-π stacking, hydrogen bonding) between the POM and the monomers guide the directional assembly of the monomers, while simultaneously confining the POM in situ within the nascent pore structure.

This approach accomplishes both framework construction and POM encapsulation in a single step, offering a more streamlined procedure, and the POM loading is usually higher than that achieved *via* the post-synthetic method. However, the presence of POM may interfere with the dynamic covalent assembly process of COF monomers, which can easily lead to a decrease in the crystallinity of COF. Therefore, it is necessary to strictly control the monomer concentration, the amount of catalyst, and the reaction temperature, in order to balance the crystallinity of the framework and the loading efficiency of POMs. Typically, POM derivatives bearing aromatic modifying groups are selected as guests; the π-π stacking between these groups and the aromatic monomers of the COF assists in ordered assembly and mitigates negative effects on crystallization. Moreover, POMs can also serve as supramolecular templates to regulate the pore size and topology of the COFs, enabling synergistic optimization of the material structure .

2.3 Overview of Comparison of the two types of materials

POM@MOFs and POM@COFs, as the mainstream confined-type POM-base catalytic systems, exhibit significant differences in their mainframe bonding nature, electronic structure, and pore channel characteristics. As a result, they show distinct variations in the loading mechanism, catalytic behavior, and environmental tolerance.

(i) Regarding loading strategies, POM@MOF systems take electrostatic interactions as the core driving force, supplemented by coordination and hydrogen bonding. Both the in situ one-pot method and the post-synthetic impregnation method have become well-established paradigms. In contrast, POM@COF systems primarily rely on supramolecular forces such as anion–π interactions and hydrogen bonding for immobilization. The mainstream approach is the post-synthetic supramolecular adsorption method, which can largely preserve framework crystallinity, but the binding strength of POM is generally weaker. Although the *in-situ* copolymerization method can increase the loading amount, it tends to interfere with the covalent assembly process and impair material crystallinity. Overall, the technological maturity of the COF-based system lags behind that of the MOF system.

(ii) In terms of catalytic activity, the two systems each excel in different scenarios. POM@MOF benefits from the acid-oxidation bifunctional synergy constructed between metal nodes and POMs, along with a pronounced confinement and enrichment effect within the pores, making it more suitable for tandem catalysis and selective transformations under mild conditions. POM@COF leverages the efficient electron transport capability of its extended conjugated skeleton and the mass transfer advantages of low-resistance straight channels, showing more significant synergistic effects in photocatalytic and electrocatalytic systems. However, due to the lack of metal active sites in the framework, its potential for bifunctional catalysis is relatively limited.

(iii) Structural stability and tolerance represent the most critical performance differentiator between the two. Under conventional reaction conditions, the covalent rigid skeleton of COFs offers better structural integrity, resulting in a lower POM leaching rate and generally longer cycling life compared to MOF coordination frameworks. In strong oxidative environments, the organic ligands in MOFs are prone to oxidative degradation, and metal nodes may leach out, leading to poor framework tolerance. In contrast, COFs employing stable linkages such as triazine can withstand harsh oxidative conditions without side reactions caused by metal leaching, thereby offering broader applicability.

Overall, MOF carriers stand out for their straightforward synthesis and diverse structural types, making them a preferred choice for developing multifunctional POM catalytic materials under mild conditions. COF carriers, with their excellent chemical stability and electron transport properties, offer irreplaceable advantages in extreme reaction environments and catalytic applications. Currently, comparisons between the two systems are largely based on scattered literature data, lacking parallel control experiments under unified reaction standards. Quantitative analysis of the structure-activity relationships still requires further in-depth

study.

3 POM@MOF-Based Catalytic System for Sulfur Oxidation

Leveraging their unique advantages, POM@MOF composite catalysts have demonstrated far superior catalytic activity and stability compared to individual components in several critical energy and environmental applications, including electrochemical CO_2 reduction, overall water splitting for hydrogen/oxygen production, fuel-cell anode desulfurization, industrial organic wastewater treatment, and degradation of persistent organic pollutants [64-68].

3.1 Overview of Synergistic Catalytic Mechanisms of POMs and MOFs

MOFs are constructed through the coordination assembly of metal-cluster nodes and organic linkers, combining the coordination activity of metal sites with the tunable functionality of organic ligands. Their synergy with POMs revolves around interfacial charge interactions, pore-confinement effects, and topology regulation.

(i) Interfacial electron-transfer synergy. Electron transfer is the core process in POM redox catalysis. The MOF skeleton can modulate the electronic structure of POMs *via* interfacial electrostatic interactions and coordination coupling, constructing directional electron-transfer channels and accelerating the catalytic cycle. For example, the positively charged, unsaturated metal nodes in MOFs (e.g., Zr^{4+}, Cu^{2+}) can form strong electrostatic attraction with the negatively charged terminal/bridging oxygen atoms on the POM surface, inducing interfacial electron rearrangement [69]. The delocalized electrons of the POM partially shift toward the metal nodes, increasing the positive charge on the POM metal centers and enhancing their activation ability toward nucleophilic substrates. Concurrently, the metal nodes can act as electron relays, lowering the energy barrier of POM redox reactions and speeding up electron transfer.

(ii) Confinement constraint and substrate-activation effects. The ordered pore cavities of MOFs can alter the adsorption behavior and reaction pathways of substrates through spatial constraints and microenvironment modulation, synergizing with the active centers of POMs. Functional groups on the pore walls can selectively concentrate substrate molecules *via* hydrophobic interactions or hydrogen bonding, significantly increasing the local substrate concentration around the POM active sites and resulting in a notable rate-enhancement effect. For instance, in ODS reactions, hydrophobic MOF channels can preferentially enrich organic sulfur substrates, enhancing the catalytic oxidation efficiency of POMs [70]. Additionally, the confined space can constrain the adsorption orientation of substrate molecules, directing the reactive sites toward the POM active centers, reducing steric hindrance, and stabilizing the reaction transition states, thereby improving the chemical and stereoselectivity of target products. Moreover, the spatial confinement of the pores can inhibit the aggregation of POM clusters, maintaining them in a monodisperse state and exposing more coordinatively unsaturated active sites. Simultaneously, the spatial constraints can finely tune the bond lengths and angles of POMs, optimize their coordination environment and boost their intrinsic catalytic activity.

(iii) Regulation *via* pore size and topology. The pore size and topological connectivity of MOFs directly determine the loading mode of POMs, the mass-transfer efficiency of substrates, and the catalytic reaction pathways, serving as central elements of structure-property relationships. Cage-type pore structures (e.g., UiO-series, ZIF-series) feature large cavities with small windows, which can completely confine POM clusters within the cages [71, 72]. The window size is smaller than the POM diameter, creating a "molecular fence" effect that spatially prevents POM leaching. Meanwhile, substrates and products can freely diffuse through the windows, ensuring catalytic progression. One-dimensional channel-type MOFs (e.g., MIL-series) exhibit low mass-transfer resistance and fast substrate diffusion, making them suitable for fast-kinetics reactions [73]; however, their binding strength for POMs is weaker than that of cage-type structures, making POM leaching more likely during long-term cycling. Three-dimensional interconnected channel MOFs possess multidirectional mass-transfer pathways, effectively mitigating concentration polarization and enhancing catalytic performance under high flow rates. Moreover, the matching degree between pore size and POM cluster size directly determines encapsulation efficiency and stability: overly large pores can cause POM aggregation, while overly small pores preclude intracavity encapsulation.

(iv) Contributions of framework defects and interfacial interactions. Intrinsic defects such as missing-linker and missing-cluster defects inevitably arise during MOF synthesis and post-treatment. These defect sites play an important regulatory role in synergistic catalysis. Defective sites usually have more unsaturated coordinated positive charge metal centers, which can form stronger electrostatic interactions with POM than the conventional skeleton sites. They can even form coordination bonds, significantly enhancing the binding strength of POM and inhibiting the loss of active components in the catalytic cycle. Furthermore, defect sites themselves can serve as Lewis acid active sites, forming bifunctional synergy with the redox-active centers of POMs. For instance, Zr^{4+} sites at defects can activate hydrogen peroxide to generate reactive oxygen species, while POMs are responsible for the oxidative transformation of substrates; the two cooperate to accelerate the reaction process [74]. The contact mode and binding distance at the interface between POMs and the MOF skeleton directly determine the electron-transfer efficiency and interaction strength, representing the core region of synergistic effects.

In the following, the research progress of sulfide catalytic conversion reaction of POM@MOFs composites will be systematically described from three application fields: catalytic synthesis of bioactive aryl sulfides, oxidative detoxification of chemical warfare agents and ODS (Table 1).

3.2 Selective Oxidation of Biologically Active Aryl Sulfides

Aryl sulfides, as an important class of organic scaffolds, are widely found in various pharmaceuticals and agrochemicals. The key values of aryl sulfides lie not only in their structural stability, but also in the sulfur atom serving as a

functionalization center for precise regulation of oxidation states. Through selective oxidation, aryl sulfides can be efficiently converted into sulfoxide or sulfone derivatives, thereby significantly altering the polarity, water solubility, and metabolic stability of the parent molecules [75-77]. This

Table 1 Summary of the research progress of representative POM@MOFs catalytic conversion of sulfur-containing compounds in recent years

Entry	Name[a]	Substrate (S content)[b]	Oxidant (O/S)[c]	*T*/°C	*t*/min	Conversion/%	Reference
1	**$PMo_{11}V$@rho-ZIF**	MPS (0.25 mmol)	H_2O_2 (1.2)	25	720	97	[78]
2	**$PMo_{10}V_2$@rho-ZIF**	MPS (0.25 mmol)	H_2O_2 (1.2)	25	720	98	[78]
3	**PMo_9V_3@rho-ZIF**	MPS (0.25 mmol)	H_2O_2 (1.2)	25	720	98	[78]
4	**$PMo^{VI/V}_{12}$@btap-MOF**	MPS (0.50 mmol)	H_2O_2 (1.2)	50	30	>99	[79]
5	**SiW_{12}@Ir-MOF**[d]	MPS (0.26 mmol)	O_2 (1 atm)	25	150	100	[80]
6	**PW_{12}@NU-1000**	CEES (0.085 mmol)	H_2O_2 (1.5)	45	180	>99	[72]
7	**PW_{12}@NU-1000-NDC**	CEES (0.085 mmol)	H_2O_2 (1.5)	45	30	>99	[81]
8	**PW_{12}@NU-1008**	CEES (0.085 mmol)	H_2O_2 (1.5)	45	30	>99	[81]
9	**PW_{12}@NU-1000-120 °C**	CEES (0.085 mmol)	H_2O_2 (1.5)	45	60	>99	[82]
10	**PW_{12}@NU-1000-$scCO_2$**	CEES (0.085 mmol)	H_2O_2 (1.5)	45	20	>99	[82]
11	**$PMo_{10}V_2$@NU-1000**	CEES (0.20 mmol)	O_2 (1 atm)	70	45	100	[83]
12	**$PMo_{10}V_2$@NU-1000-120 °C**	CEES (0.20 mmol)	O_2 (1 atm)	70	45	100	[83]
13	**$PMo_{10}V_2$@NU-1000-$scCO_2$**	CEES (0.20 mmol)	O_2 (1 atm)	70	45	100	[83]
14	**$MnMo_6$@PCN-601**	CEES (0.30 mmol)	H_2O_2 (1.5)	25	10	>99	[84]
15	**$PMo_{10}V_2$@MIL-101**	SM (0.034 mmol)	O_2 (1 atm)	25	120	97.39	[85]
16	**$PMo_{10}V_2$@MOF-808**	CEES (0.034 mmol)	O_2 (1 atm)	25	120	93.91	[86]
17	**BW_{12}@HKUST-1**	CEES (0.25mmol)	H_2O_2 (1.5)	25	10	100	[87]
18	**PW_9@MIL-101**	DBT* (1707 mg·L^{-1})	H_2O_2 (~9.0)	50	120	100	[88]
19	**PMo_4@MIL-101**	DBT* (2000 mg·L–1)	H_2O_2 (~3.0)	70	120	100	[89]
20	**$PW_{11}Zn$@NH_2-MIL-101**	DBT* (~1500 mg·L^{-1})	H_2O_2 (~8.0)	50	360	100	[90]
21	**$Eu(PW_{11})_2$@NH_2-MIL-53**	DBT* (~2500 mg·L^{-1})	H_2O_2 (23.0)	70	120	100	[91]
22	**PW_{12}@MIL-101-SiO_2**	DBT* (500 mg·L^{-1})	H_2O_2 (5.0)	60	120	98.6	[92]
23	**PMo_{12}@MIL-100**	DBT* (2000 mg·L^{-1})	H_2O_2 (~8.0)	70	30	100	[70]
24	**PMo_4@MOF-808**	DBT* (2000 mg·L^{-1})	H_2O_2 (~3.0)	70	120	73.1	[89]
25	**PMo^V_4@MOF-808**	DBT* (2000 mg·L^{-1})	H_2O_2 (9.0)	70	60	99.5	[93]
26	**$PW_{11}Zn$@MOF-808**	DBT* (500 mg·L^{-1})	H_2O_2 (5.0)	50	30	99.4	[69]
27	**PW_4@UiO-67**	DBT* (500 mg·L^{-1})	H_2O_2 (~25.0)	70	40	99.6	[94]
28	**PW_{12}@UiO-66**	DBT* (1000 mg·L^{-1})	H_2O_2 (3.0)	30	25	99.9	[95]
29	**IL-PMo_{12}@UiO-66**	DBT* (500 mg·L^{-1})	H_2O_2 (3.0)	80	20	100	[74]
30	**Mo_6W_6@NH_2-UiO-66**[d]	DBT* (250 mg·L^{-1})	TBHP (~6.7)	25	100	99	[96]
31	**Mo_6W_6@HKUST-1**[d]	DBT* (250 mg·L^{-1})	TBHP (~6.7)	25	100	80	[96]
32	**PMo_9V_3@rht-MOF-1**	DBT* (1000 mg·L^{-1})	H_2O_2 (12.0)	70	50	96	[97]
33	**$PW_{11}V$@rht-MOF-1**	DBT* (1000 mg·L^{-1})	H_2O_2 (12.0)	70	50	87	[98]
34	**$PW_{10}V_2$@rht-MOF-1**	DBT* (1000 mg·L^{-1})	H_2O_2 (12.0)	70	50	89	[98]
35	**PW_9V_3@rht-MOF-1**	DBT* (1000 mg·L^{-1})	H_2O_2 (12.0)	70	50	98	[98]
36	**$P_2Mo_{16}V_2$-CNTs@HKUST-1**	DBT* (200 mg·L^{-1})	O_2 (1 atm)	60	240	92.245	[99]

[a]According to the structural characteristics, the samples were uniformly named in this review; [b]DBT*refers to a mixture of DBT and its derivatives; [c]O/S refers to the molar ratio of oxidant to sulfur element; [d]Photocatalytic system (the rest are thermal catalytic system).

strategy provides a direct route for optimizing the pharmacokinetic properties of lead compounds. Particularly noteworthy is that sulfoxide and sulfone groups themselves frequently act as critical pharmacophores contributing directly to biological activity, typical examples include the proton pump inhibitor omeprazole (a sulfoxide) and the antileprotic drug dapsone (a sulfone) [100-102]. Meanwhile, the construction of chiral sulfoxide structures has also opened new dimensions for developing highly selective bioactive molecules. Therefore, using aryl sulfides as precursors to construct diverse sulfur-containing functional groups *via* oxidation has become a key strategy in modern drug design for enhancing activity, improving druggability, and expanding chemical space.

Zeolitic Imidazolate Frameworks (ZIFs), a highly representative subclass of the MOF family, occupy a

prominent position in porous materials research due to their unique topological isomorphism and physicochemical properties [103, 104]. The most distinctive structural feature of ZIFs lies in their geometric configuration, which is highly similar to that of traditional inorganic aluminosilicate zeolites. It is precisely this topological analogy that enables ZIFs to construct tetrahedral networks (such as SOD, LTA, etc.) akin to those of zeolites, thereby endowing the materials with the dual advantages of both the high porosity of MOFs and the high stability of inorganic zeolites. Compared to traditional MOFs, ZIFs exhibit exceptional thermal and chemical stability. Many ZIF materials not only maintain their framework integrity at high temperatures but also demonstrate good resistance to hydrolysis and collapse even in boiling water, strong bases, or organic solvents. Furthermore, the synthesis conditions for ZIFs are generally mild, with some materials preparable at room temperature *via* solvothermal or aqueous-phase methods, aligning with green chemistry principles. Simultaneously, by introducing different functional groups onto the imidazole rings, precise control over pore size and channel chemical environment can be achieved, greatly expanding their applications in gas adsorption, separation, and catalysis. Consequently, ZIFs have become one of the ideal platforms for constructing high-performance functional composites like POM@MOFs.

Hu et al. successfully synthesized a highly crystalline host-guest-type POM-based rho-ZIF *via* a one-pot mechanochemical method. This metastable rho-ZIF possesses enormous internal cavities and pore windows, serving as an ideal host matrix for the efficient loading and robust anchoring of large-sized vanadium-substituted Keggin-type POM ($PMo_{12-n}V_n$ = $H_{n+3}PMo_{12-n}V_nO_{40}$) molecules through physical confinement **($PMo_{12-n}V_n$@rho-ZIF)** [78]. Experiments confirm that the guest molecules were effectively locked within the host framework without compromising its integrity, preventing the leaching of active components. As a novel heterogeneous catalyst, the **$PMo_{12-n}V_n$@rho-ZIF** composites exhibit pronounced catalytic activity in the selective oxidation of sulfides to sulfoxides (Fig. 1(a)). Leaching experiments verify the heterogeneous nature of the catalytic process, and the catalysts show no significant loss in activity after four cycles. Notably, this work pioneers the use of large-pore metastable rho-ZIF for encapsulating sizable guest molecules, providing an efficient and versatile new strategy for designing confined catalytic systems with highly dispersed and stable catalytic centers.

Liu's group employed the multidentate nitrogenous azole ligand (btap) to prepare two novel POM@MOF composites (**$PMo^{VI/V}_{12}$@btap-MOF**, $PMo^{VI/V}_{12}$ = $[HPMo^{VI}_{10}Mo^{V}_{2}O_{40}]^{4-}$) with well-defined crystalline structures *via* a one-pot hydrothermal method under mild conditions [79]. Single-crystal X-ray diffraction analysis confirmed that the two compounds are isostructural. Within their crystal structures, metal ions coordinate with the btap ligands, assembling into left-handed and right-handed helical one-dimensional chains. These chains connect in a twisted and alternating fashion, ultimately constructing a three-dimensional MOFs featuring two-fold interpenetration. The POM anions are *in-situ* encapsulated within the channels generated by this interpenetrated structure, achieving highly dispersed and stable immobilization of the POM active sites within the framework. Catalytic performance reveals that, using hydrogen peroxide as a green oxidant, both compounds demonstrated true heterogeneous catalytic activity and high sulfoxide selectivity in the selective oxidation of sulfides (Fig. 1(b)). In particular, in the selective oxidation of methyl phenyl sulfide (MPS), the catalyst could completely convert MPS to methyl phenyl sulfoxide (MPSO) within 30 min, with the selectivity for the target product exceeding 99%. The catalytic system also demonstrates good substrate scope, effectively catalyzing the selective transformation of various aryl sulfides into their corresponding sulfoxide products. Notably, these catalysts exhibit good recyclability. After at least five catalytic runs, the yield of the target sulfoxide products shows no significant decrease, indicating that the materials possess both pronounced catalytic activity and structural stability.

With the growing global energy demand and the increasing depletion of traditional energy sources, the search for efficient, environmentally friendly, and sustainable energy has become a crucial topic in scientific research. Photocatalysis, as a green technology capable of directly utilizing solar energy to drive chemical reactions, demonstrates significant potential in

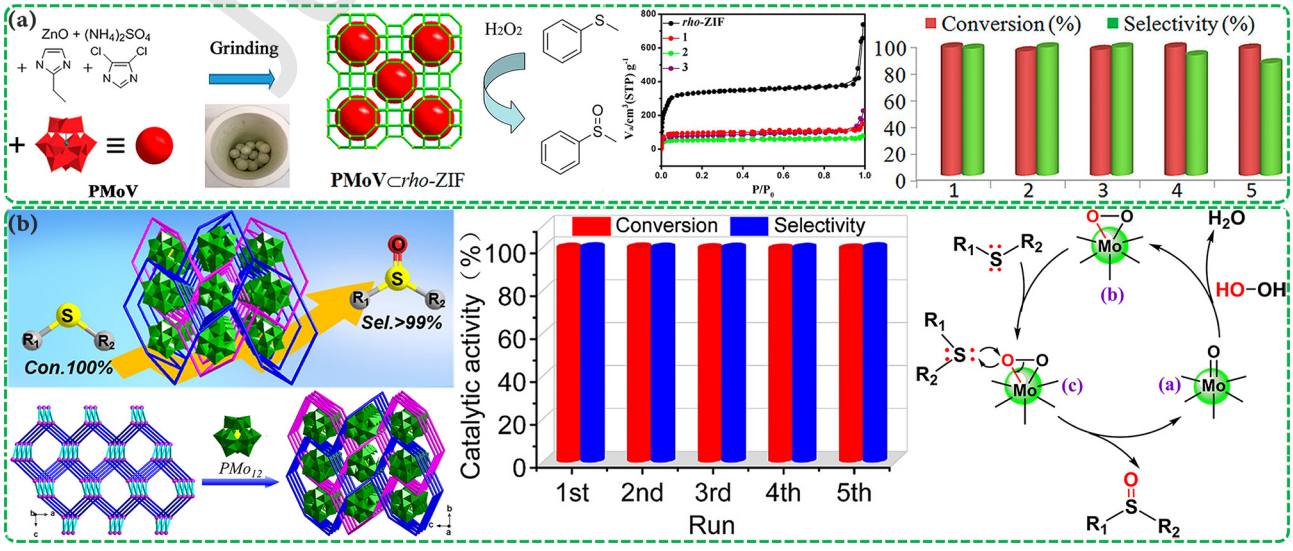

Figure 1 (a) Schematic preparation route of **$PMo_{12-n}V_n$@rho-ZIF**, isothermal adsorption curves before and after loading, and catalytic cycle stability. Reproduced with permission from Ref. [78], © American Chemical Society 2017. (b) Structure of **$PMo^{VI}{}_{12-n}V^{V}_{n}$@btap-MOF**, catalytic cycle stability and catalytic mechanism. Reproduced with permission from Ref. [79], © American Chemical Society 2023

addressing both the energy crisis and environmental pollution [105-107]. The unique properties of POMs also render them promising for photocatalytic applications [66, 108]. However, POMs typically absorb only ultraviolet light, and their limited light absorption range restricts their catalytic performance under visible light. To extend their absorption spectrum, the introduction of additional photosensitizers is required to enhance light utilization efficiency. In recent years, a strategy of constructing POM@MOF photocatalytic systems by incorporating metal-based photosensitizers into MOFs developed by Lin, Zhang, and others, has been recognized as an effective improvement approach and has been widely adopted [45, 109, 110].

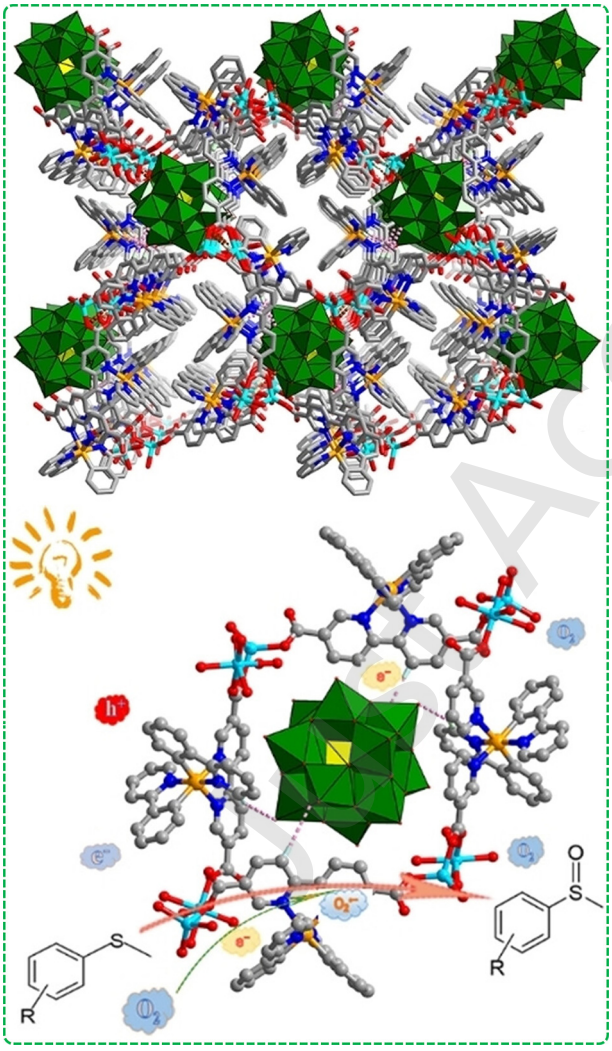

Figure 2 Structure of **SiW_{12}@Ir-MOF** and schematic illustration of photocatalytic oxidation of aryl sulfides. Reproduced with permission from Ref. [80], © Wiley-VCH GmbH. 2023.

Following a similar innovative strategy, Niu et al. recently successfully constructed a crystalline POM@MOF composite photocatalyst (**SiW_{12}@Ir-MOF**, SiW_{12} = $[SiW_{12}O_{40}]^{4-}$), *via* a one-step self-assembly approach using functionalized iridium (Ir) metal ligands and Keggin-type silicotungstic acid [80]. By incorporating Ir metal ligands possessing strong metal-to-ligand charge transfer absorption characteristics, this material successfully extends the light-response range from the ultraviolet region into the visible light spectrum, significantly improving the effective utilization of solar energy. More importantly, under visible light irradiation (λ > 400 nm), photogenerated electrons from the excited-state Ir metal ligands can be rapidly transferred to adjacent SiW_{12} units *via* the interface. This effectively suppresses bulk recombination of photogenerated charge carriers, substantially enhancing the efficiency of charge carrier separation and transport. Benefiting from the synergistic effect between the visible-light harvesting capability of the Ir metal ligands and the redox catalytic ability of the POM units, **SiW_{12}@Ir-MOF** exhibits satisfactory photocatalytic activity and selectivity in the selective oxidation of sulfides. Under mild reaction conditions, with only 2.5 h of visible light irradiation, the yield of the target product, MPSO, reaches 99.5% (Fig. 2). This catalytic performance is markedly superior to that of most POM-based composite photocatalysts that had been reported at that time. Furthermore, the catalyst demonstrates good structural stability and recyclability. After three consecutive catalytic cycles, the yield of MPSO remains above 97% with no significant loss of activity. This study provides a new design paradigm for constructing POM-based composite photocatalysts with efficient visible-light response and offers important experimental support for advancing the practical application of photocatalytic technology in fine organic synthesis and green chemical engineering.

3.3. Catalytic Oxidation Detoxification Chemical Warfare Agents

Chemical warfare agents (CWAs) are a class of toxic chemical substances that achieve personnel incapacitation and ecological destruction through toxicological effects [111-113]. Due to their immense destructive power and long-lasting deterrent effects, CWAs have always been a central focus of research in the fields of international security and protective science. Among them, the blister agent SM is widely regarded as the "king of CWA" because of its simple synthesis process, low production cost, and severe injury consequences. Developing efficient and rapid detoxification and degradation technologies for SMs is a critical issue to be addressed in the fields of chemical defense medicine and environmental safety [114-116]. Among various degradation strategies, chemical oxidative degradation is considered one of the most effective and widely applied methods. Its core mechanism lies in attacking the thioether bond in the SM molecule with strong oxidants, thereby altering its electronic structure to eliminate its alkylating activity [116-118]. Currently, many oxidative systems represented by hypochlorites, H_2O_2, and POMs have been extensively studied, aiming to achieve rapid and complete degradation under mild conditions [4, 119].

Zr-MOFs exhibit unique thermal and chemical stability, maintaining structural integrity even in strong acids, strong bases, and boiling water environments. Their typical hexanuclear zirconium cluster secondary building units confer a rigid framework to the material, and the highly tunable structure

allows for precise regulation of pore environments and defect sites. By virtue of the dual advantages of ultrahigh stability and rich functionality, Zr-MOFs have emerged as highly promising frontier carriers for constructing POM-based composite

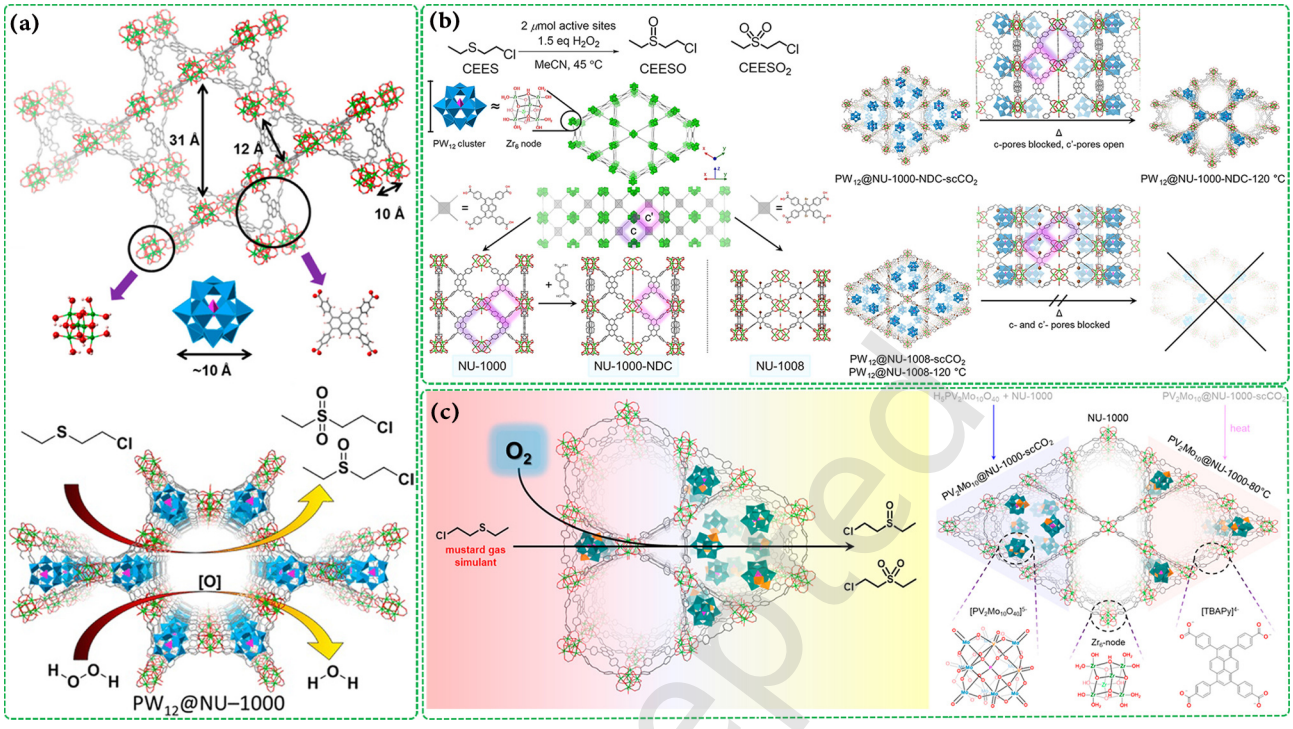

Figure 3 (a) Structure of **PW_{12}@NU-1000** and schematic illustration of H_2O_2-mediated oxidative CEES degradation. Reproduced with permission from Ref. [72], © American Chemical Society 2017. (b) Schematic illustration of the preparation of **PW_{12}@NU-1000-NDC** and **PW_{12}@NU-1008**, as well as their activation in 120 °C and $scCO_2$. Reproduced with permission from Ref. [81], © Frontiers Media SA. 2019. (c) Structure of **$PMo_{10}V_2$@NU-1000** and its activation in 80 °C and $scCO_2$, as well as schematic illustration of O_2-mediated oxidative CEES degradation. Reproduced with permission from Ref. [83], © American Chemical Society 2019.

materials (POM@MOF). Farha's group has achieved fruitful results in the encapsulation of POMs within the NU series of Zr-MOFs and applied them to the rapid oxidative decontamination of 2-chloroethyl ethyl sulfide (CEES). Using NU-1000 as a foundation, the researchers prepared **PW_{12}@NU-1000** (PW_{12} = $H_3PW_{12}O_{40}$) *via* a conventional strategy (Fig. 3(a)) [72]. To further optimize its catalytic activity, the team attempted several modification strategies. The first was pore channel modification, preparing **PW_{12}@NU-1000-NDC** by introducing naphthalene dicarboxylic acid (NDC). The second was structural confinement, constructing a migration-blocking composite material, **PW_{12}@NU-1008**, by utilizing the NU-1008 carrier to restrict POM migration [81]. Furthermore, they compared different activation methods, preparing thermal activation-type (at 120 °C) and supercritical carbon dioxide ($scCO_2$) activation-type series of materials (Fig. 3(b)) [81, 82]. In the CEES oxidation system using H_2O_2 as the oxidant, the catalytic activity of the aforementioned POM@MOF composite materials is significantly superior to that of each individual component, confirming the synergistic effect between the POM active sites and the MOF carrier. Experimental results show that the initial turnover frequency (TOF) of **PW_{12}@NU-1000** was 10.4 min^{-1}; the activity of **PW_{12}@NU-1000-120 °C** after thermal activation improved slightly to 11.4 min^{-1}; whereas the activity of the $scCO_2$-activated **PW_{12}@NU-1000-$scCO_2$** exhibited a qualitative leap, with its TOF approximately three times that of the thermally activated sample. A similar trend applied to the NDC-modified and NU-1008 systems, i.e., the TOFs of the $scCO_2$-activated samples were superior to their thermally activated counterparts.

Subsequently, the group extended the research to an aerobic oxidation system, encapsulating divanadium-substituted $PMo_{10}V_2$ into NU-1000 (**$PMo_{10}V_2$@NU-1000**) (Fig. 3(c)) [83]. Results indicated that in the CEES reaction using O_2 as the oxidant, $scCO_2$ activation could still significantly enhance catalytic performance. Studies revealed that $scCO_2$ activation facilitates the uniform distribution of POMs within the micro- and mesoporous channels of MOFs, thereby increasing the contact probability between substrates and active sites and accelerating the catalytic process.

Metal cluster catalysts, characterized by atomically precise active sites, unique electronic structures, and quantum size effects, exhibit broad application prospects in various catalytic reactions, including energy conversion, environmental remediation, and fine chemical synthesis. However, simultaneously maximizing the catalytic activity of metal clusters while enhancing their structural stability remains a long-standing core challenge in this field. To address this critical scientific issue, Wu and co-workers innovatively proposed a dual-cluster POM@MOFs construction strategy. Through a size-matched ligand exchange reaction, they precisely co-localized Ni sites derived from the defective MOF framework and Mo sites originating from POM clusters within a sub-nanometer confined pocket, successfully fabricating a stable dual-cluster POM@MOF catalyst, **$MnMo_6$@PCN-601** ($MnMo_6$ = $[H_6MnMo_6O_{24}]^{4-}$), featuring atomically synergistic bimetallic sites (Fig. 4(a)) [84]. This design strategy not only

utilizes the rigid MOF skeleton to achieve spatial isolation and stable immobilization of the metal clusters but, more importantly, constructs a bimetallic active center with strong electronic interactions *via* sub-nanoscale site co-localization.

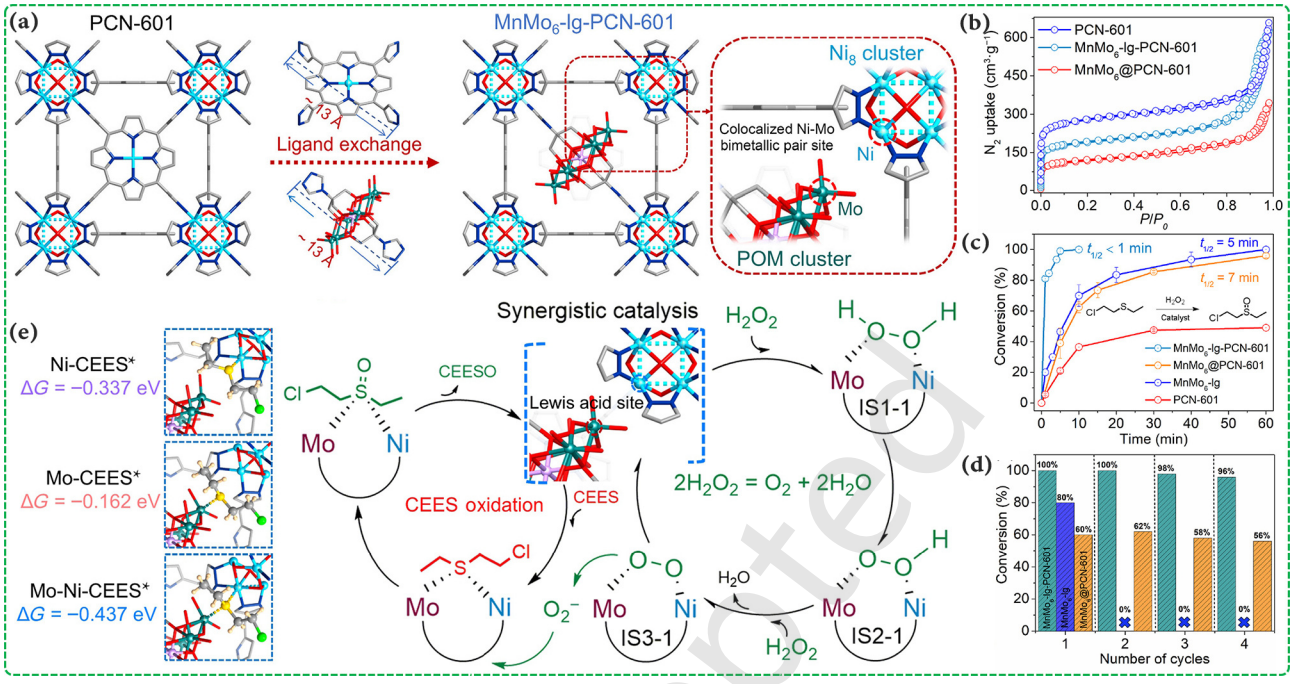

Figure 4 (a) Structure of **MnMo$_6$@PCN-601**. (b) Isothermal adsorption curves before and after loading **MnMo$_6$@PCN-601**. (c) Catalytic performance of CEES degradation. (d) Catalytic cycle stability. (e) Catalytic mechanism. Reproduced with permission from Ref. [84], © Tsinghua University Press Ltd. and SciOpen 2025.

Catalytic performance evaluation revealed that **MnMo$_6$@PCN-601** exhibits significantly superior comprehensive performance compared to traditional single-component catalysts in the oxidative degradation of the chemical warfare agent simulant CEES. The reaction half-life is less than 1 min, with a TOF as high as 140 min^{-1}, alongside satisfactory structural stability and recyclability (Fig. 4(b-d)). The catalytic mechanism is elucidated through combined *in-situ* Fourier-transform infrared spectroscopy and density functional theory calculations. A significant atomically synergistic effect exists between the co-localized Ni-Mo bimetallic sites (Fig. 4(e)). On one hand, this dual-site synergy strengthens the adsorption and activation process of the CEES substrate. On the other hand, it effectively promotes the decomposition of the oxidant H_2O_2 to generate reactive oxygen species, thereby achieving the efficient and selective oxidative degradation of CEES. This work provides a novel design paradigm for tackling the classic activity-stability trade-off in metal cluster catalysts and opens a new research direction for developing efficient catalytic materials suitable for complex reaction systems involving multiple substrates.

Zhang et al. also focused on the good performance of $PMo_{10}V_2$ in sulfide oxidation reactions and loaded it onto two typical metal-organic frameworks, MOF-808 and MIL-101(Cr), using the classical impregnation method [85, 86]. The results show that the composite material **PMo$_{10}$V$_2$@MIL-101** could effectively catalyze the selective oxidation of CEES to 2-chloroethyl ethyl sulfoxide (CEESO) under mild conditions. More importantly, this material also demonstrates effective decontamination capability against the real chemical warfare agent SM. Under room temperature and atmospheric pressure, only 20 mg of the catalyst was required to eliminate 97.39% of CEES (approximately 30 μmol) within 120 min [85]. Mechanistic studies reveal that the system follows an adsorption-oxidation synergistic mechanism, that is, MIL-101(Cr) rapidly enriches the toxic agent within its pores due to its high specific surface area, and the highly dispersed $PMo_{10}V_2$ active sites then achieve complete detoxification. Additionally, the **PMo$_{10}$V$_2$@MOF-808** also exhibits unique bifunctional catalytic activity. This material not only degraded 93.91% of CEES within 120 min (with a half-life of 27.77 min) but also achieved complete hydrolysis of the nerve agent simulant methyl paraoxon within 25 min (100% decontamination, with a half-life of only 1.895 min) [86]. Recycling tests confirm that the composite maintained stable decontamination activity after four cycles. This high decontamination performance is attributed to the synergistic effect of dual active sites. $PMo_{10}V_2$ confined within the pores catalyzes the selective oxidation of CEES, while the unsaturated metal sites on the MOF-808 framework promote the catalytic hydrolysis of DMNP, enabling efficient simultaneous purification of two different types of toxic agents (Fig. 5).

NENU-n series POM@MOFs are hybrid materials constructed by encapsulating a series of high-performance Keggin-type POMs into the $Cu_3(BTC)_2$ framework (HKUST-1) [120]. They exhibit broad application prospects in fields like catalysis and proton conduction. Addressing the technical bottleneck that Keggin-type tungsten-based POMs have relatively weak oxidation capability, making it difficult to synthesize pure-phase **NENU-n** hybrid products in situ on copper substrates, Liu et al. built upon previous work and developed a novel strategy for the *in-situ* synthesis of POM@MOFs on copper foil. By introducing oxygen into the

acidic reaction system, oxygen oxidizes elemental copper on the surface of the copper foil to divalent copper ions, which

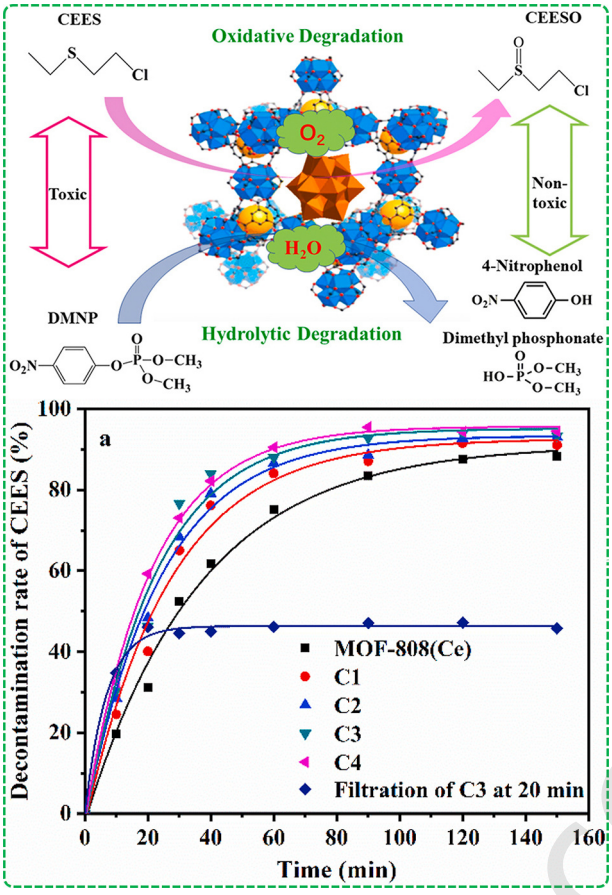

Figure 5 Structure of **$PMo_{10}V_2$@MOF-808** and schematic catalytic oxidation degradation of CEES. Reproduced with permission from Ref. [86], © Elsevier Ltd. 2021.

hybrid materials of the series on copper substrates. The method can be carried out at room temperature, offering significant advantages such as simple operation, fast reaction, and high atom economy. More importantly, the synthesis system does not require any additional morphology-regulating agents to achieve controllable morphology synthesis of POM@MOFs. The final morphology shows a clear structure-activity relationship with the charge number of the POM anions. High-charge polyoxoanions induce the formation of cubic-shaped products, whereas low-charge polyoxoanions correspond to octahedral-shaped products. Using the catalytic oxidation reaction of the mustard gas simulant CEES as a performance evaluation model, studies confirmed that the cubic-shaped **NENU-40** (**BW_{12}@HKUST-1**, BW_{12} = $K_5BW_{12}O_{40}$) material exhibits optimal catalytic activity because it can expose more catalytic active sites. It can completely convert CEES into the non-toxic sulfoxide product CEESO within 10 min [87].

3.4. Catalytic Oxidation Desulfurization

Desulfurization of fuel oil has always been a core subject and key technological step in the process of fuel cleaning and refining. Hydrodesulfurization, as the most mature mainstream desulfurization technology currently applied industrially, is widely used for the removal of sulfur-containing compounds (eg, serve as the copper source for the growth of the MOFs. This successfully achieved the *in-situ* preparation of pure-phase benzothiophene (BT), dibenzothiophene (DBT), 4,6-dimethyldibenzothiophene (4,6-DMDBT)) from fuel oil, with related research having undergone decades of development and refinement [121, 122]. However, as global environmental standards for fuel oil become increasingly stringent, hydrodesulfurization technology faces severe technical bottlenecks. Its effectiveness in removing refractory organic sulfur compounds, such as thiophene derivatives, is significantly challenged, and it suffers from inherent drawbacks, including high-temperature and high-pressure operation, high hydrogen consumption, and elevated operational costs [123]. In this context, non-hydrodesulfurization technologies have experienced rapid development in recent years. Among various emerging non-hydrodesulfurization technologies, ODS has emerged as one of the most promising desulfurization technologies for industrial application, owing to its notable advantages, such as mild reaction conditions, no requirement for a hydrogen source, and high efficiency in Removing refractory organic sulfur compounds [124-126]. POMs have been extensively and deeply studied in the field of oxidative desulfurization [127, 128]. To address the core issues of POMs in homogeneous systems, such as easy dissolution in the reaction medium, difficulty in recovery and reuse, and poor cycling stability, encapsulating and confining POMs within the channels of mesoporous molecular sieves has become one of the mainstream modification strategies. Related research has achieved abundant results and significant progress over the past few decades [3, 129].

MIL series metal-organic frameworks (such as MIL-53 and MIL-101) are highly favored in heterogeneous catalysis due to their unique chemical robustness, large pore volume, and high specific surface area. It is generally accepted in the literature that the encapsulation of POMs within MIL-101(Cr) represents the first example in this field, successfully integrating the activity of homogeneous catalysis with the easy separation characteristics of heterogeneous catalysis [73]. Leveraging the synergistic catalytic effect between the MIL framework and POMs, such composite materials not only effectively concentrate and activate reactants but also optimize electron transfer pathways, thereby significantly enhancing catalytic rates and cycling stability. This opens a new avenue for the development of high-performance catalytic systems.

Substantial research contributions have been made by Balula and co-workers in the realm of incorporating POMs into MIL-series MOFs and leveraging these composites for ODS processes. By employing a diverse array of lacunary and substituted Keggin-type POMs as catalytically active centers, the research group has successfully synthesized a broad spectrum of POM@MIL heterogeneous catalysts tailored for ODS reactions. Within composite systems utilizing MIL-101(Cr) as the supporting matrix, the investigators sequentially achieved the stable immobilization of both the trilacunary Keggin-type POM ($[A\text{-}PW_9O_{34}]^{9-}$, PW_9) and the highly catalytically active peroxo-molybdate species ($[PMo_4O_8(O_2)_8]^{3-}$, PMo_4). Notably, the **PW_9@MIL-101** catalyst enables thorough desulfurization of a model oil feedstock with an initial sulfur content of 1707

mg/L within 120 min under ambient temperature conditions (Fig. 6(a)) [88]. Furthermore, this composite material facilitates the quantitative conversion of geraniol to 2,3-epoxygeraniol in as little as 30 min, with the rigid MOF framework markedly

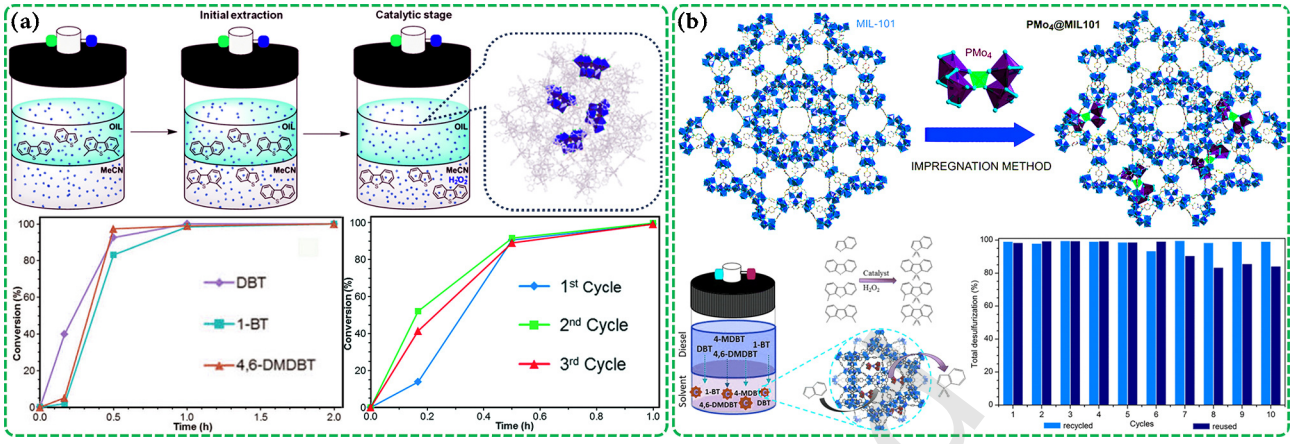

Figure 6 (a) Schematic catalytic oxidative desulfurization of **PW_9@MIL-101**, catalytic performances of different substrates and stability of catalytic cycle. Reproduced with permission from Ref. [88], © Royal Society of Chemistry 2014. (b) Structure of **PMo_4@MIL-101** and stability of catalytic cycle in oxidative desulfurization. Reproduced with permission from Ref. [89], © Royal Society of Chemistry 2023.

augmenting the structural stability of PW_9 in hydrogen peroxide-containing reaction media. The **PMo_4@MIL-101** catalyst, in turn, exhibits superior performance in the ODS treatment of a multi-component model diesel fuel, achieving complete sulfur elimination within 120 min and retaining consistent catalytic activity over 10 consecutive reaction cycles (Fig. 6(b)) [89]. In-depth mechanistic investigations reveal that the window dimensions and pore diameter of the MOF support play a critical role in determining the overall catalytic performance of the composites. Owing to its well-suited porous architecture, MIL-101 effectively facilitates the mass transport of reactant molecules while simultaneously suppressing the leaching of active POM species. To further expand the repertoire of viable MOF supports and optimize catalytic efficacy, the research team shifted their focus to aluminum-based MOFs, pioneering the application of amino-functionalized NH_2-MIL-101(Al) and NH_2-MIL-53(Al) in the fabrication of ODS catalysts. Through a combined synthetic strategy involving one-pot microwave-mediated synthesis and wet impregnation, the team successfully encapsulated the monosubstituted lacunary $[PW_{11}Zn(H_2O)O_{39}]^{5-}$ ($PW_{11}Zn$) within the pore cavities of NH_2-MIL-101(Al), yielding the **$PW_{11}Zn$@NH_2-MIL-101** composite [90]. When coupled with ionic liquid extraction technology, this catalyst achieves near-complete desulfurization of model diesel under mild reaction conditions, and also delivers an 83% sulfur removal efficiency when tested against real diesel fuel samples. Additionally, the composite catalyst prepared by immobilizing the sandwich-type POM ($[Eu(PW_{11}O_{39})_2]^{11-}$, $Eu(PW_{11})_2$) onto NH_2-MIL-53(Al) (**$Eu(PW_{11})_2$@NH_2-MIL-53**) also displayed remarkable ODS activity, achieving deep desulfurization of model fuel within 120 min and significantly outperforming the homogeneous $PW_{11}Eu$ catalyst [91]. The structural intactness of both the POM active sites and the MOF frameworks in all aforementioned composite catalysts was verified through a comprehensive suite of characterization techniques. No appreciable decline in catalytic activity or detectable leaching of active components is observed after multiple reaction cycles, providing valuable experimental insights and theoretical guidance for the rational design of high-performance heterogeneous oxidation catalysts.

In recent years, the functional modification of the benchmark MIL-101(Cr) support, pioneered by Su et al., has become one of the most prominent and rapidly developing research areas in heterogeneous ODS catalysis. To tackle the long-standing challenge of insufficient POM dispersion in hydrophobic oil phases, the team devised a novel hierarchical confinement strategy by embedding PW_{12} decorated MIL-101(Cr) nanoparticles into the interconnected mesoporous channels of diatomaceous earth, yielding a novel ternary **PW_{12}@MIL-101-SiO_2** composite catalyst [92]. The natural diatomite scaffold serves as both a robust mechanical support and an efficient adsorbent for organic sulfides, creating a local high-concentration environment around the active sites and enhancing mass transfer efficiency. With H_2O_2 as the green oxidant, the catalyst delivers a remarkable desulfurization performance of 98.6%, and X-ray diffraction analysis confirms that its crystalline structure was well preserved after three successive runs.

Motivated by the need to develop cost-effective and industrially viable catalytic processes, Balula's research group shifted their attention to the earth-abundant MIL-100(Fe) support and established an integrated green protocol for the simultaneous removal of sulfur and nitrogen compounds from fuels. Conventional hydrodesulfurization technologies suffer from high energy consumption and operational costs, and nitrogen-containing compounds are known to severely poison desulfurization catalysts. To address these issues, the researchers synthesized a **PMo_{12}@MIL-100** composite by encapsulating Keggin-type $H_3PMo_{12}O_{40}$ (PMo_{12}) within the MIL-100(Fe) cavities (Fig. 7(a)) [70]. Through a synergistic combination of catalytic oxidation and liquid-liquid extraction, complete removal of all refractory sulfur and nitrogen species from a complex multi-component model fuel was accomplished in just 30 min (Fig. 7(b)). A major advantage of this system is the use of inexpensive ethanol as the extractant instead of costly ionic liquids such as $[BMIM]PF_6$, which dramatically reduces the

overall process economics without compromising purification efficiency. The solid catalyst and the ethanol extractant could be recycled for multiple cycles; however, after the fourth cycle, the oxidation desulfurization property significantly declined. This might be due to the difficulty in extracting sulfur-containing compounds from the fuel phase to the ethanol phase (Fig. 7(c)).

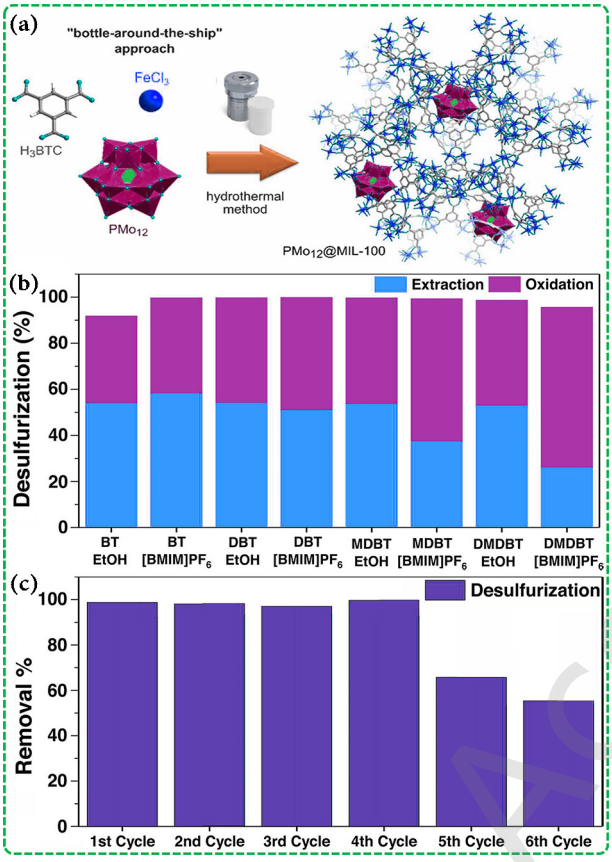

Figure 7 (a) Schematic synthesis route and structure of **PMo_{12}@MIL-100**. (b) Oxidative extraction desulfurization for different substrates and different solvents. (c) Cyclic stability of ODS and oxidative denitrification reaction. Reproduced with permission from Ref. [70], © Elsevier Ltd. 2023.

Balula et al. had benchmarked their material against **PMo_4@MOF-808**, which was found to deliver only subpar ODS performance, with a maximum desulfurization efficiency of 73.1% recorded after 120 min of reaction [89]. Building on this foundation, Zhao et al. recently revisited the **PMo_4@MOF-808** system with the aim of unlocking its full catalytic potential. Employing a single set of precursors, they synthesized one structurally related composite with reduced oxidation states (**PMo^{V}_4@MOF-808**) through an *in-situ* solvothermal reduction process (Fig. 8(a)) [93]. Extraction-coupled ODS experiments reveal that the reduced pentavalent molybdenum catalyst exhibited dramatically enhanced activity, achieving near-complete desulfurization of model oil in just 60 min, which far surpass that of the hexavalent molybdenum analog. A comprehensive analysis combining experimental characterization and density functional theory calculations attribute this remarkable improvement to the uniform spatial distribution of active sites within the MOF porous network and the superior electron-donating ability of pentavalent Mo centers, which significantly accelerate the rate-determining electron transfer step (Fig. 8(a)).

Recognizing the limitations of bare MOF-808 as an ODS catalyst, Haruna et al. developed a green one-pot solvothermal encapsulation technique to incorporate $PW_{11}Zn$ into MOF-808, producing a series of **$PW_{11}Zn$@MOF-808** composites with tunable loadings [69]. Structural characterization confirmed that $PW_{11}Zn$ clusters were successfully embedded and homogeneously dispersed throughout the MOF-808 framework without disrupting its inherent crystallinity. Catalytic evaluation uncovered a remarkable synergistic interaction between the $PW_{11}Zn$ guest and the MOF-808 host (Fig. 8(b)). Under optimized mild conditions, the **$PW_{11}Zn$@MOF-808** composite achieves 99.40% DBT conversion in 30 min, representing a 14.5% increase in activity compared to pristine MOF-808 (86.85%). The catalyst shows substrate-dependent activity, with the following order of sulfur removal efficiency: DBT > BT > 4,6-DMDBT. More importantly, the **$PW_{11}Zn$@MOF-808** composite also maintains decent structural stability and catalytic performance over eight consecutive reaction cycles, with no significant leaching of active components detected, highlighting its potential for practical industrial applications.

Zirconium-based MOFs belonging to the UiO series have garnered significant attention as superior platforms for constructing high-performance POM-derived ODS catalysts, owing to their unparalleled combination of adjustable pore architectures, versatile surface functionalization capabilities, and precisely engineered defect structures. Capitalizing on the host-guest size complementarity principle, Zhao's group developed a one-pot *in-situ* fabrication approach to confine the Venturello-type polyoxoanions clusters ($[PW_4O_8(O_2)_8]^{3-}$, PW_4) within the nanoscale cavities of UiO-67(Zr), resulting in the formation of the **PW_4@UiO-67** composite [94]. The hierarchical porous structure of UiO-67 not only possesses ideal pore diameters and restricted pore windows, but also performs two functions. Firstly, it uses its framework to in-situ fix individual POM molecules, preventing leaching. Secondly, it forms a restricted reaction microenvironment, thereby promoting the oxidation kinetics of various organic sulfur substrates. Remarkably, this catalyst achieves near-complete removal of four notoriously refractory sulfur compounds (BT, DBT, and 4,6-DMDBT) in just 30 min, and retained more than 85% of its initial activity after 10 successive reaction runs.

In a groundbreaking study, Ye and collaborators introduced a revolutionary defect engineering paradigm to synthesize UiO-66(Zr)-supported POM catalysts (**PW_{12}@UiO-66**) with systematically varied defect densities through a room-temperature pore modulation technique [95]. Their work unequivocally demonstrates that the undercoordinated Zr defect sites in UiO-66 are the critical active centers that enable efficient ODS catalysis at room temperature, with catalytic Performance scaling linearly with defect density. The most active defect-rich catalyst achieves 100% desulfurization of a 1000 mg/L model oil in only 25 min at ambient temperature, and exhibits an unprecedented TOF value of 620.0 h^{-1} at 30 °C, setting a new benchmark for MOF-based ODS catalysts. Complementary DFT simulations provide atomic-level insights into the synergistic mechanism, revealing that the

hydroxyl and aqua ligands attach to the exposed Zr defect sites act as efficient H_2O_2 activators, generating reactive hydroperoxyl species that rapidly convert to the catalytically essential peroxo-polyoxoaions intermediates.

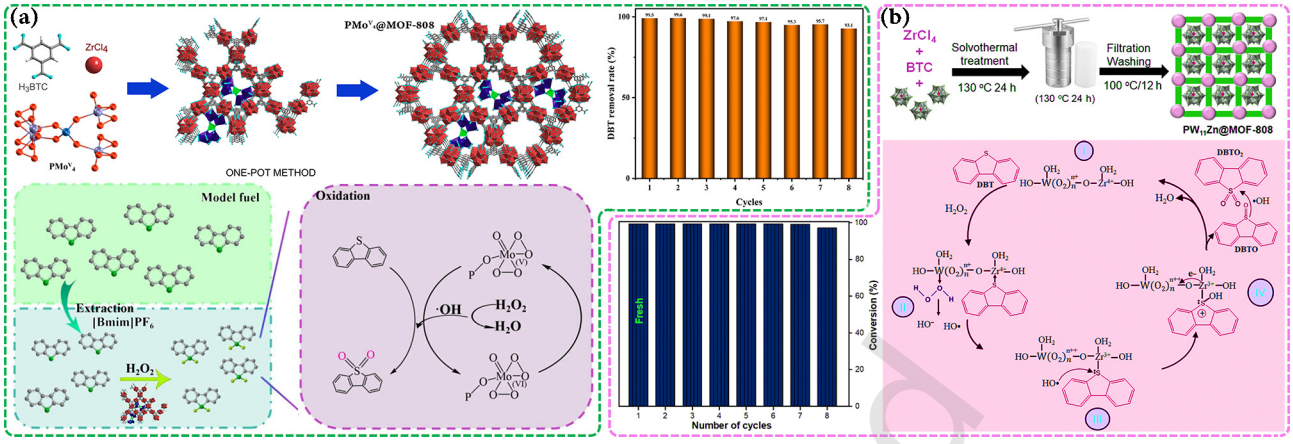

Figure 8 (a) Schematic illustration of catalytic oxidative desulfurization of **PMo^{V}_4@MOF-808**, catalytic performances of different substrates and stability of catalytic cycle. Reproduced with permission from Ref. [93], © Elsevier Ltd. 2026. (b) Schematic synthesis route and structure of **$PW_{11}Zn$@MOF-808**, and stability of catalytic cycle in oxidative desulfurization. Reproduced with permission from Ref. [69], © Elsevier Ltd. 2023.

Drawing on the similar strategies of omission mentioned above, Bu et al. recently employed the bottle-around-ship assembly strategy and successfully synthesized the **IL-PMo_{12}@UiO-66** (IL-PMo_{12} = $[Bmim]_3PMo_{12}O_{40}$) composite catalyst through one-pot post-modification technology (Fig. 9(a)) [74]. They innovatively introduced thiourea to achieve dual regulation. On one hand, thiourea releases CO_2, NH_3 and H_2S gases under acidic heating conditions, creating ligand defects during the UiO-66 synthesis process, generating a large number of Zr(IV) unsaturated coordination sites and oxygen vacancies that can capture electrons; on the other hand, the released H_2S acts as a reducing agent, efficiently reducing phosphomolybdic acid to heteropoly blue, with a Mo^{5+}/Mo^{6+} molar ratio as high as 2. Moreover, combined with the cation modification of POMs by ionic liquids, the electrophilic nature of the imidazolium ring can enhance the adsorption capacity of the substrate. The ODS catalytic performance test indicates that the activity of the composite catalyst is much higher than that of pure POM and pure MOF, with the reaction rate constant for 4,6-DMDBT reaching 4.155 s^{-1}. This high activity stems from the strong adsorption of the imidazolium ring on the electron-rich 4,6-DMDBT, effectively overcoming the spatial steric hindrance of the 4,6-alkyl substituents. Additionally, a higher proportion of Mo^{5+} active sites in the system is more easily activated by the oxidant TBHP, generating hydroxyl radical active species, thereby significantly enhancing the catalytic activity. After 6 cycles of catalyst usage, the DBT conversion still remained at 100%, while the 4,6-DMDBT conversion remained at approximately 95% and 82% respectively; the crystal structure, heteropoly blue valence state and Keggin structure of the catalyst did not undergo significant changes after the reaction, demonstrating good cycle stability.

The Farzadkia research group loaded the bimetallic Keggin-type $H_3[PMo_6W_6O_{40}]$ (Mo_6W_6) onto amino-modified zirconium-based MOF (NH_2-UiO-66) and copper-based MOF (HKUST-1). Through hydrothermal method, they prepared **Mo_6W_6@NH_2-UiO-66** and **Mo_6W_6@HKUST-1** composites, and applied them to the simultaneous oxidation removal of DBT and quinoline in diesel under visible light LED irradiation [96]. The band gap of the composite materials was significantly narrower than that of pure POMs, and the visible light absorption capacity was significantly improved. The catalytic performance tests showed that **Mo_6W_6@NH_2-UiO-66** exhibited better catalytic activity, achieving a 99% DBT removal rate and a 99% quinoline removal rate within 100 min, and its performance was significantly superior to **Mo_6W_6@HKUST-1**. Although the authors did not provide a specific explanation for the performance differences between the two, we speculate that this might be due to the introduction of amino groups enhancing the adsorption ability of the substrates. The underlying reason still needs to be further confirmed through subsequent research.

Moving beyond the well-established MOF supports reviewed earlier, numerous research groups have pushed the boundaries of catalyst design by exploring MOFs with unconventional topologies and carbon nanotube (CNT)-reinforced MOF hybrid supports for POM-based ODS applications. By implementing sophisticated design strategies such as precise host-guest dimensional matching and targeted vanadium doping of POM active centers, these novel catalysts have demonstrated markedly improved performance in treating real fuel feedstocks. In a landmark study, Li's research team harnessed the exceptional cage-like porous structure of rht-MOF-1 to encapsulate a family of vanadium-substituted Keggin phosphomolybdates within its internal cavities [97]. Single-crystal XRD analysis verified that the resulting composites achieved exceptionally high POM loadings while maintaining remarkable chemical stability (Fig. 9(b)). This catalyst series exhibited robust desulfurization activity across both model diesel formulations and actual commercial diesel samples. The standout performer, **PMo_9V_3@rht-MOF-1**, delivers desulfurization efficiencies of 96% for model oil and 90% for real diesel. This exceptional performance stems from a powerful synergistic effect: the moderately sized rht-MOF-1 cages act as molecular sieves to prevent POM leaching, while the Keggin POM clusters provide abundant accessible active sites for the oxidation of

recalcitrant sulfur species including DBT, BT, and 4,6-DMDBT. Building on this success, the same group extended their approach to vanadium-substituted Keggin phosphotungstates, synthesizing a series of **$PW_{12-n}V_n$@rht-MOF-1** (($PW_{12-n}V_n$ =

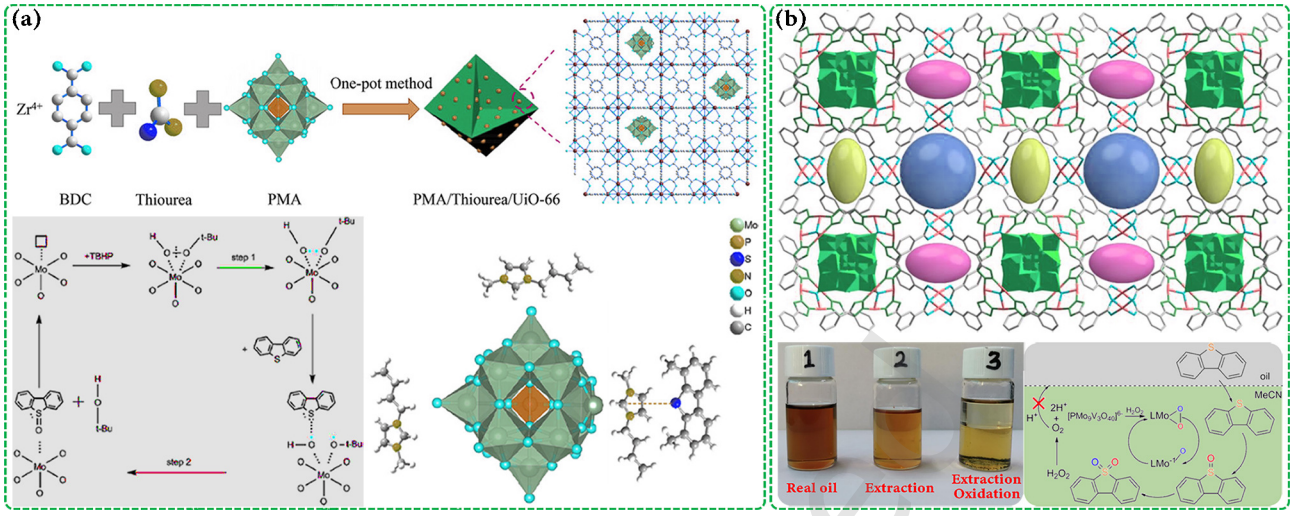

Figure 9 (a) Schematic synthesis route and structure of **IL-PMo_{12}@UiO-66** and possible oxidation mechanism. Reproduced with permission from Ref. [74], © Wiley-VCH GmbH. 2020. (b) Structure of **PMo_9V_3@rht-MOF-1**, desulfurization for real oil, and possible oxidation mechanism. Reproduced with permission from Ref. [97], © Elsevier Ltd. 2020.

$H_{n+3}PW_{12-n}V_nO_{40}$)) composites [98]. Under optimized conditions, the best-performing catalyst achieves impressive removal efficiencies for a mixed-sulfide model oil. Through detailed kinetic analysis, electron paramagnetic resonance spectroscopy, and radical scavenging experiments, the authors elucidate a free radical-mediated reaction pathway and confirmed the recyclability of the catalyst.

In a parallel effort to address mass transfer and electron conductivity limitations in traditional MOF supports, Zhao et al. developed an innovative CNTs@MOF-199 hybrid support and employed a one-pot synthesis strategy to immobilize a range of vanadium-substituted Dawson-type POMs, yielding a family of ternary composite catalysts [99]. Extensive characterization confirmed the successful formation of the hybrid materials, with POM active species uniformly distributed throughout the CNT-MOF matrix. Catalytic testing reveals that vanadium substitution plays a critical role in modulating activity, with **$P_2Mo_{16}V_2$-CNTs@HKUST-1** ($P_2Mo_{16}V_2$ = $H_8P_2Mo_{16}V_2O_{62}$) emerging as the optimal catalyst, achieving 98.30% DBT conversion under optimized conditions. Kinetic analysis demonstrates that the reaction follows pseudo-first-order kinetics with an impressively low apparent activation energy of 12.89 kJ/mol. Furthermore, the catalyst retains nearly full activity after multiple consecutive cycles, highlighting its exceptional structural stability.

4 POM@COF-Based Catalytic System for Sulfur Oxidation

As a new type of composite material in recent years, POM@COF has attracted much attention. This section aims to explore the design of high-performance composite materials based on host-guest synergistic effects. To comprehensively cover relevant research, a broad definition is adopted, incorporating porous aromatic frameworks (PAFs), covalent organic polymers (COPs), and other porous frameworks with covalent linkage characteristics into the discussion. Emphasis is placed on their encapsulation of POM molecules and their catalytic oxidation applications in sulfur-containing compounds.

4.1 Overview of Synergistic Catalytic Mechanisms of POMs and COFs

COFs are constructed through the directional covalent condensation of organic monomers, featuring long-range ordered conjugated frameworks, precisely tunable pore structures, and excellent chemical stability. Their synergy with POMs centers on conjugated-framework electron coupling, rigid-pore confinement, and supramolecular interfacial interactions, exhibiting distinct synergistic characteristics that differ from MOF-based systems.

(i) Conjugated framework-mediated electron-transfer synergy. COFs possess long-range delocalized π-electron systems that can serve as continuous electron-conducting pathways, forming efficient charge-transport networks with POMs. This represents the most distinctive synergistic feature distinguishing them from MOF systems. Unlike the node-based electron transfer in MOFs, the two-dimensional conjugated layers or three-dimensional conjugated frameworks of COFs enable rapid electron migration among multiple POM active sites, effectively preventing charge recombination and the isolation of active sites. For instance, in photocatalytic systems, conjugated COFs can act as photosensitizing units, absorbing visible light to generate photogenerated charge carriers [33]. Photogenerated electrons are rapidly injected into the lowest unoccupied molecular orbital of POMs through interfacial anion-π interactions, significantly enhancing the reduction capability of POMs. Simultaneously, POMs serve as multi-electron reservoirs that efficiently capture photogenerated electrons, suppressing the recombination of electron-hole pairs and prolonging carrier lifetimes.

(ii) Confinement activation and mass-transfer synergy in rigid pores. COFs feature uniform pore sizes, strong structural rigidity, and precisely modifiable pore-wall functional groups, making their confinement effects more regular and stable

compared to those of MOFs. First, the one-dimensional straight channels of COFs exhibit extremely low mass-transfer

Table 2 Summary of the research progress of representative POM@COFs catalytic conversion of sulfur-containing compounds in recent years

Entry	Name[a]	Substrate (S content)[b]	Oxidant (O/S)[b]	*T*/°C	*t*/min	Conversion/%	Reference
1	**PW_{12}@TpPa-1**	MPS (0.50 mmol)	H_2O_2 (1.3 mmol)	60	60	99.5	[130]
2	**PMo_{12}@TpPa-1**	MPS (0.50 mmol)	H_2O_2 (1.3 mmol)	60	60	92.6	[130]
3	**SiW_{12}@TpPa-1**	MPS (0.50 mmol)	H_2O_2 (1.3 mmol)	60	60	89.4	[130]
4	**PW_{12}@RT-COF-1**	MPS (0.50 mmol)	H_2O_2 (1.3 mmol)	50	120	99.9	[131]
5	**SiW_{12}@RT-COF-1**	MPS (0.50 mmol)	H_2O_2 (1.3 mmol)	50	120	47	[131]
6	**PMo_{12}@RT-COF-1**	MPS (0.50 mmol)	H_2O_2 (1.3 mmol)	50	120	49.5	[131]
7	**SiW_{12}@CTF**[d]	MPS (0.20 mmol)	O_2 (1 atm)	25	120	97	[132]
8	**PW_{12}@CTF**[d]	MPS (0.20 mmol)	O_2 (1 atm)	25	120	89	[132]
9	**PMo_{12}@CTF**[d]	MPS (0.20 mmol)	O_2 (1 atm)	25	120	36	[132]
10	**PW_{12}@Ag-COF**[d]	MPS (0.10 mmol)	O_2 (1 atm)	25	210	98	[133]
11	**PW_{12}@Cu-COF**[d]	MPS (0.10 mmol)	O_2 (1 atm)	25	210	54	[133]
12	**PW_{12}@Ni-COF**[d]	MPS (0.10 mmol)	O_2 (1 atm)	25	210	87	[133]
13	**K-SiW_{12}@PCP**[d]	MPS (0.20 mmol)	O_2 (1 atm)	25	16	>99	[134]
14	**K-PW_{12}@PCP**[d]	MPS (0.20 mmol)	O_2 (1 atm)	25	16	92	[134]
15	**K-SiW_{11}@PCP**[d]	MPS (0.20 mmol)	O_2 (1 atm)	25	16	94	[134]
16	**K-SiW_{10}@PCP**[d]	MPS (0.20 mmol)	O_2 (1 atm)	25	16	88	[134]
17	**K-SiW_9@PCP**[d]	MPS (0.20 mmol)	O_2 (1 atm)	25	16	78	[134]
18	**D-$P2W_{18}$@PCP**[d]	MPS (0.20 mmol)	O_2 (1 atm)	25	18	>99	[135]
19	**D-$P2Mo_{18}$@PCP**[d]	MPS (0.20 mmol)	O_2 (1 atm)	25	18	92	[135]
20	**SiW_{12}@CTF**[d]	CEES (0.20 mmol)	O_2 (1 atm)	25	60	98	[132]
21	**PW_{12}@CTF**[d]	CEES (0.20 mmol)	O_2 (1 atm)	25	60	78	[132]
22	**PMo_{12}@CTF**[d]	CEES (0.20 mmol)	O_2 (1 atm)	25	60	24	[132]
23	**PW_{12}@Ag-COF**[d]	CEES (0.10 mmol)	O_2 (1 atm)	25	120	>99	[133]
24	**PW_{12}@Cu-COF**[d]	CEES (0.10 mmol)	O_2 (1 atm)	25	120	16	[133]
25	**PW_{12}@Ni-COF**[d]	CEES (0.10 mmol)	O_2 (1 atm)	25	120	48	[133]
26	**K-SiW_{12}@PCP**[d]	CEES (0.20 mmol)	O_2 (1 atm)	25	8	99	[134]
27	**K-PW_{12}@PCP**[d]	CEES (0.20 mmol)	O_2 (1 atm)	25	8	90	[134]
28	**K-SiW_{11}@PCP**[d]	CEES (0.20 mmol)	O_2 (1 atm)	25	8	92	[134]
29	**K-SiW_{10}@PCP**[d]	CEES (0.20 mmol)	O_2 (1 atm)	25	8	86	[134]
30	**K-SiW_9@PCP**[d]	CEES (0.20 mmol)	O_2 (1 atm)	25	8	74	[134]
31	**D-$P2W_{18}$@PCP**[d]	CEES (0.20 mmol)	O_2 (1 atm)	25	10	99	[135]
32	**D-$P2Mo_{18}$@PCP**[d]	CEES (0.20 mmol)	O_2 (1 atm)	25	10	94	[135]
33	**Mo_8@PAF-1**	DBT* (500 mg·L^{-1})	H_2O_2 (6.0)	30	30	98.2	[136]
34	**PMo_{12}@PAF-54**	DBT* (800 mg·L^{-1})	H_2O_2 (4.0)	40	45	100	[137]
35	**PMo_4V_8@iPAF-1**	DBT* (500 mg·L^{-1})	O_2 (1 atm)	80	300	100	[138]
36	**IMo_6@iPAF-1**	DBT* (500 mg·L^{-1})	O_2 (1 atm)	90	300	100	[56]
37	**PMo_4V_8@iPAF-270**	DBT* (1000 mg·L^{-1})	H_2O_2 (7.0)	60	100	98.2	[139]
38	**$CoMo_6$@iPAF-30**	DBT* (500 mg·L^{-1})	Air (1 atm)	130	60	100	[140]

[a]According to the structural characteristics, the samples were uniformly named in this review; [b]DBT*refers to a mixture of DBT and its derivatives; [c]O/S refers to the molar ratio of oxidant to sulfur element; [d]Photocatalytic system (the rest are thermal catalytic system).

resistance. Substrate molecules can rapidly diffuse to POM active sites within the channels, while products can quickly desorb and exit, effectively avoiding product-inhibition effects and enhancing the kinetic rate of catalytic reactions. Second, the shape-selective effect of rigid pores is significant, allowing only substrates with matching sizes and conformations to enter the channels and contact POM active centers. This enables precise molecular recognition and selective catalysis, particularly suitable for reactions such as the selective transformation of isomers. Third, weak-interaction sites on COF pore walls (e.g., triazine rings, imine bonds, hydroxyl groups) can form hydrogen bonds, π-π stacking, and other weak interactions with substrate molecules, assisting in the pre-activation of substrates and creating "dual-site cooperative activation" with the redox-active centers of POMs.

(iii) Structure-property regulation *via* pore size and topology. The pore sizes of COFs can be precisely tuned at the atomic level by varying the length of organic monomers, and the channels are highly ordered. Their topological structures are mainly divided into two-dimensional layered pores and three-dimensional interconnected pores. Two-dimensional COFs primarily feature one-dimensional straight channels with a wide tunable pore-size range. POMs can be uniformly loaded inside the channels, and interlayer anion-π interactions can further enhance POM stability. These are currently the dominant systems in POM@COF research. However, their layered structures are prone to stacking under extreme conditions, leading to channel blockage and the burial of active sites. Three-dimensional COFs possess three-dimensionally interconnected pore structures and higher specific surface areas, enabling complete encapsulation of POMs within the 3D pore network. They combine the advantages of binding stability and mass-transfer efficiency, but their synthesis is challenging, crystallization control is difficult, and related catalytic studies are still in the early stages. Moreover, topology also determines the spatial distribution of pore-wall functional groups, thereby influencing the loading density and dispersion uniformity of POMs, ultimately regulating catalytic activity.

(iv) Interfacial supramolecular interactions and defect effects. Unlike MOF systems where interfacial binding is primarily electrostatic, COF frameworks are overall electrically neutral. Their interfacial binding with POMs relies mainly on supramolecular interactions such as anion-π interactions, hydrogen bonds, and van der Waals forces. The type and strength of interfacial interactions directly determine the loading stability of POMs and synergistic efficiency. Defects in COFs mainly include crystalline defects, unreacted terminal-group defects, and bonding defects. Among these, unreacted terminal groups such as amino or aldehyde groups can become positively charged through protonation, serving as strong adsorption sites for POMs and enhancing POM loading capacity and stability. Moreover, the covalent frameworks of COFs exhibit higher chemical stability. Their interfacial structures are less susceptible to damage under harsh reaction conditions such as strong acids, strong bases, or strong oxidizing environments, ensuring the long-term persistence of synergistic effects. This represents a prominent advantage over MOF-based systems.

In the following, the research progress of sulfide catalytic conversion reaction of POM@COFs composites will be systematically described from three application fields: catalytic synthesis of bioactive aryl sulfides, oxidative detoxification of chemical warfare agents and ODS (Table 2).

4.2. Selective Oxidation of Biologically Active Aryl Sulfides

Using a mechanochemical approach, Wang et al. achieved the *in-situ* immobilization of Keggin-type PW_{12} within the TpPa-1 under solvent-free conditions at room temperature (Fig. 10(a)) [130]. This synthetic route not only fully preserves the intrinsic structure of the POMs but also, by leveraging the spatial confinement effect of the TpPa-1 carrier, ensures sufficient exposure of active sites. Simultaneously, strong electrostatic interactions significantly enhance the structural stability of the active components, offering a new paradigm for the green synthesis of POM-based catalysts. In the oxidation of sulfides under mild conditions, **PW_{12}@TpPa-1** with a loading of 27% showed the most obvious effect, achieving complete conversion of MPS within 60 min and yielding sulfone products with high selectivity (99%). Studies indicate that the satisfactory performance originates from the synergistic activation of substrates by the active sites. This composite material integrates the high activity of homogeneous catalysis with the easy separation characteristic of heterogeneous catalysis.

Recently, the team employed the room-temperature ion exchange method to load typical Keggin-type POMs onto the room-temperature synthesized cationic RT-COF-1, thereby preparing a series of POMs@RT-COF-1 composite materials. Among them, **PW_{12}@RT-COF-1** achieved the optimal loading amount and pore channel filling effect (Fig. 10(b)) [131]. The formed II-type heterojunction could significantly promote the separation and transfer of photogenerated carriers, and the electrochemical impedance test shows that its charge transfer resistance was the lowest. The catalytic performance indicates that at 50 °C, with ultrasound assistance and H_2O_2 as the oxidant under mild conditions, **PW_{12}@RT-COF-1** achieves a 99.9% MPS conversion and 100% $MPSO_2$ selectivity within 120 min, and its performance is significantly higher than that of **SiW_{12}@RT-COF-1** and **PMo_{12}@RT-COF-1**. This catalyst exhibits extensive substrate universality, with conversion and selectivities exceeding 90% for most aryl and aliphatic sulfides, and is slightly reduced only by large steric hindrance substituents. It also possesses fine cycle stability, with the catalytic activity and selectivity remaining basically unchanged after 4 cycles. The active species capture experiment and band analysis revealed that the acoustic luminescence generated by ultrasound cavitation and the local hot spot activation of the catalyst decomposed H_2O_2 to generate active free radicals, with photogenerated electrons transferring from the conduction band of RT-COF-1 to the conduction band of PW_{12} and dominating the reaction, while holes, superoxide free radicals, and hydroxyl free radicals cooperatively participated.

COFs also represent a prominent class of emerging photocatalytic materials, whose uniquely tunable molecular-level electronic properties grant them significant photocatalytic advantages [107, 112, 141]. Their highly adjustable band structures can effectively optimize the light absorption range (covering visible to near-infrared regions) and enhance redox kinetics. Meanwhile, the extensively delocalized π-conjugated system facilitates directional transport of photogenerated charge carriers, significantly boosting catalytic efficiency by suppressing charge recombination. As electron acceptors and active centers, the introduction of POMs substantially enhances the oxidative capability of the system [142, 143]. In POM@COF heterostructures, synergistic electronic interactions at the interface promote the transfer of photogenerated electrons from the excited state of the COF to the POM clusters [33]. This synergistic effect integrates the strong light-harvesting ability of COFs with the high redox activity of POMs, exhibiting an

exhibit performance beyond that of individual components in photocatalytic reactions involving multi-electron transfer.

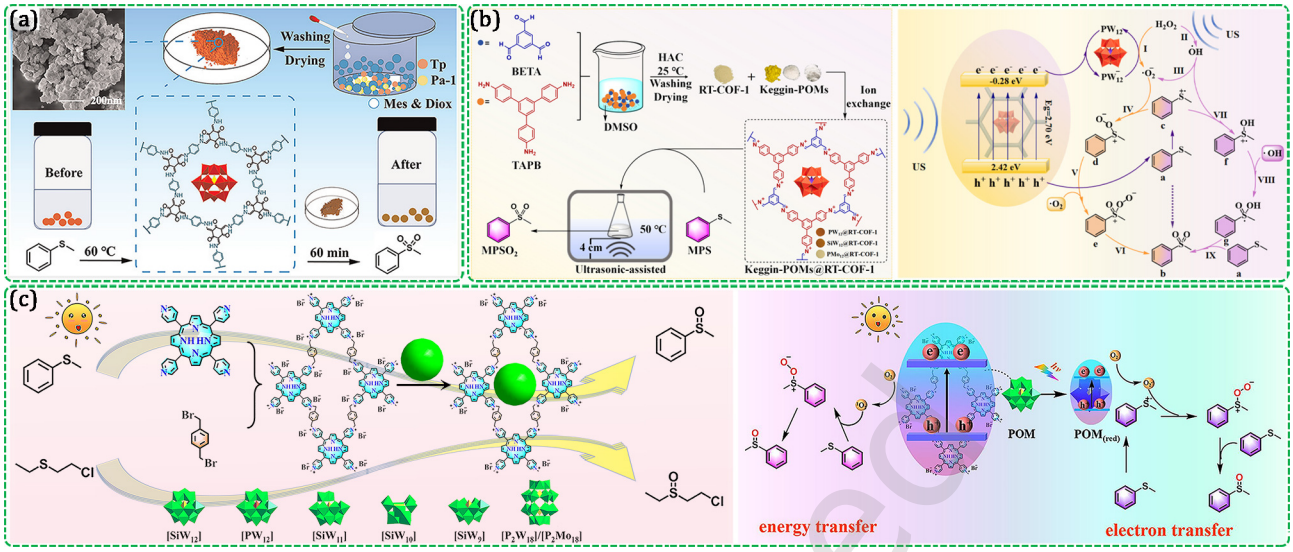

Figure 10 (a) Structure of **PW_{12}@TpPa-1** and catalytic performance in MPS oxidation. Reproduced with permission from Ref. [130], © Royal Society of Chemistry 2023. (b) Schematic synthesis route and structure of **PW_{12}@RT-COF-1** and the possible oxidation mechanism assisted by ultrasound. Reproduced with permission from Ref. [131], © Elsevier Ltd. 2026. (c) Structure of **POM@PCP**, catalytic performance in MPS oxidation and CEES degradation, and catalytic mechanism of the dual reaction path. Reproduced with permission from Ref. [134, 135], © Elsevier Ltd. 2024 and © American Chemical Society 2025.

In recent years, the An's group has conducted a series of in-depth studies in this field. Using a hydrothermal synthesis strategy, they encapsulated different Keggin-type POMs (e.g. SiW_{12}, PW_{12}, PMo_{12}) as guest components into covalent triazine frameworks (CTFs). Under 10 W 425 nm LED illumination in an oxygen atmosphere, this series of POM@CTF composites exhibit satisfactory performance in the selective photooxidation of various sulfides to the corresponding sulfoxides [132]. Among them, **SiW_{12}@CTF** shows the highest activity, achieving efficient conversion of MPS within 120 min (conversion >97%, selectivity >99%). Structure-activity relationship studies reveal that the strongly electronegative, oxygen-rich POM components can effectively construct built-in electric fields, inducing differentiated electron transfer behaviors, thereby significantly promoting charge carrier separation and migration.

The team also further attempted to enhance performance by functionalizing the COF backbone. By introducing metal ions (M-COFs) into a COF containing bipyridine units, they prepared a **PW_{12}@M-COF** system [133]. Experiments confirmed that the type of metal ion significantly modulates the activity, with Ag^+-modified **PW_{12}@Ag-COF** showing the best performance (98% MPS conversion within 3.5 h). Recently, they integrated strongly light-absorbing porphyrin units and N^+-containing viologen-like units (PCP) into the framework. They also used ion exchange technology to systematically introduce a series of POM active centers with different structures and activities, covering saturated and lacunary Keggin-type POMs (K-POMs) and classical Dawson-type POMs (D-POMs), and then prepared a series of encapsulated POM-based composites (**K-POM@PCP** and **D-POM@PCP**) (Fig. 10(c)) [134, 135]. Benefiting from the strong visible-light harvesting ability of porphyrin and the heavy-atom effect of the POMs, these systems (especially **K-SiW_{12}@PCP** and **D-P_2W_{18}@PCP**) exhibit extremely high catalytic kinetics, accomplishing near-quantitative conversion of MPS (99%) within 16-18 min. Mechanistic studies confirm that the reaction follows a dual-path synergistic mechanism involving electron transfer and energy transfer, driven jointly by superoxide radicals ($\cdot O_2^-$) and singlet oxygen ($^1O_2$) for efficient substrate conversion. Particularly, D-POMs, with their abundant active sites, effectively broadened the spectral response range and accelerated charge separation. In summary, this series of studies successfully constructed POM-based photocatalytic systems featuring broad spectral response, high activity, and good stability, not only providing new insights for the design of high-performance composite photocatalysts but also offering technical support for the value-added conversion of sulfides driven by visible light.

4.3. Catalytic Oxidation Detoxification Chemical Warfare Agents

The series of composite materials prepared by An et al., as mentioned earlier, including **SiW_{12}@CTF**, **PW_{12}@Ag-COFs**, and **POM@PCP**, have demonstrated noteworthy catalytic performance in the oxidative detoxification of SM simulant (2-chloroethyl ethyl sulfide, CEES) (Fig. 10(c)) [132-135]. **SiW_{12}@CTF** achieves 98% CEES conversion within 60 min under room temperature and 10W 425nm LED illumination (1 atm O_2), with a selectivity of up to 99% for the low-toxicity product (CEESO). Although the activity of **PW_{12}@Ag-COFs** was slightly lower than expected, it still achieves efficient degradation within 120 min, significantly outperforming its counterparts modified with Cu^{2+} or Ni^{2+}. Thanks to the incorporation of porphyrin photosensitive units, porphyrin-based composites (**K-POM@PCP** and **D-POM@PCP**) exhibited good photocatalytic activity. Under optimal conditions, **D-P_2W_{18}@PCP** required only 10 min to achieve 99% conversion and >99% CEESO selectivity, while **K-SiW_{12}@PCP**

further reduced the degradation time to 8 min, setting a leading standard in the field at the time. The exceptional

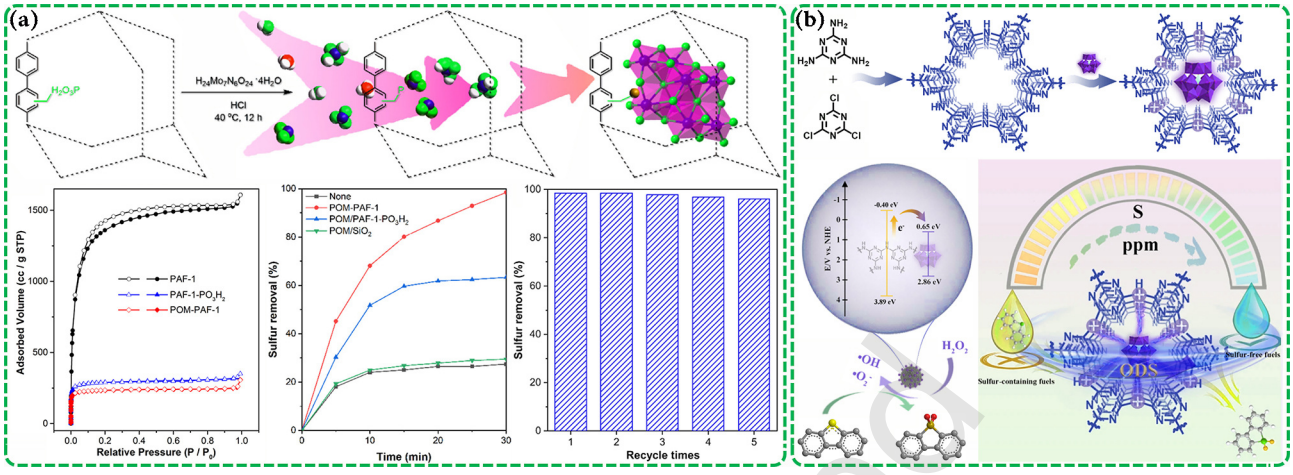

Figure 11 (a) Schematic synthetic route, isothermal adsorption desorption curve, catalytic performance and cycle stability of **Mo_8@PAF-1**. Reproduced with permission from Ref. [136], © American Chemical Society 2020. (b) Schematic synthetic route and catalytic mechanism of **PMo_{12}@PAF-54**. Reproduced with permission from Ref. [137], © Science China Press and Springer Nature 2024.

catalytic performance of these materials is primarily attributed to synergistic effects. The porphyrin structural units endowed the composites with acceptable visible-light harvesting capabilities, while the POMs, leveraging their strong electronegativity and heavy-atom effects, significantly suppressed the recombination of photogenerated charge carriers and accelerated charge separation. This enhancement in electron and energy transfer processes ultimately greatly improved the overall efficiency of photocatalytic degradation.

4.4. Catalytic Oxidation Desulfurization

PAFs constitute a family of three-dimensionally cross-linked porous polymers, synthesized *via* robust covalent linkages between rigid aromatic monomers [59, 144]. The combination of their ultra-high specific surface area, remarkable thermochemical robustness, precisely engineered pore architectures, and versatile functionality enables broad utility in gas storage, heterogeneous catalysis, and separation technologies. Regarding POM immobilization, the dense aromatic domains within PAFs facilitate the uniform dispersion and anchoring of POM species, effectively mitigating aggregation and leaching. Concurrently, the intrinsically hydrophobic framework minimizes interference from polar solvents at active sites, thereby bolstering catalytic stability and recyclability; furthermore, the unique pore confinement effects can synergistically enhance reaction selectivity. Consequently, PAFs are deemed superior scaffolds for fabricating high-performance supported POM catalytic systems. To date, PAF-based POM composites have been predominantly explored for ODS applications.

Pioneering work by Zhu, Tian, et al. introduced phosphonic acid moieties onto PAF-1, followed by the *in-situ* entrapment of polyoxomolybdate clusters ($[Mo_8O_{26}]^{4-}$, Mo_8) *via* a "ship-in-a-bottle" approach to yield the hybrid catalyst **Mo_8@PAF-1** (Fig. 11(a)) [136]. This material demonstrates exceptional ODS performance, achieving 98.5% removal of DBT under mild conditions (30 °C, 30 min), alongside fine substrate generality for thiophene (TP), BT, and 4,6-DMDBT. Mechanistic investigations reveal that strong interfacial interactions between Mo_8 and the $-PO_3H_2$ groups ensured high dispersion of the active phase, while the host matrix high porosity and lipophilicity significantly optimized mass transfer kinetics.

Pan et al. have recently introduced a sophisticated ODS catalytic system that leverages phosphomolybdic acid (PMo_{12}) supported on a reductive PAF-54 framework. This study represents a convergence of multiple design principles such as tailored pore architecture, high-loading anchoring, the regulation of amphiphilicity and the enhancement of activity *via* a reductive framework, resulting in a remarkable leap in the performance of the **PMo_{12}@PAF-54** composite (Fig. 11(b)) [137]. The performance evaluation show that the catalyst could promote the rapid and complete oxidation of DBT in the model oil within 30 min in the H_2O_2-driven ODS reaction under mild reaction conditions. It also shows similar catalytic activity for BT and 4,6-DMDBT, which can effectively achieve deep green desulfurization of fuel oil. Notably, its catalytic activity outperforms the vast majority of existing POM-based ODS catalysts. The system also exhibits good recyclability, maintaining full desulfurization efficiency after six consecutive cycles. The core innovation lies in moving beyond the traditional paradigm of inert carriers to systematically elucidate a dual synergistic host-guest mechanism. On one hand, PAF-54's high specific surface area ensures the high dispersion of PMo_{12} active sites, and its unique amphiphilicity effectively lowers interfacial mass transfer resistance. On the other hand, the reductive skeleton induces electron transfer and rearrangement within the PMo_{12}, forming active reducing species (Mo^{5+}) that fundamentally enhance the intrinsic activity of the catalytic component. Additionally, the study underscores the versatility of nitrogen-rich porous organic polymers for reductive applications. Consequently, this work not only provides a rational, multifunctional synergistic strategy for designing ODS catalysts but also pioneers a new pathway for applying host-guest electron regulation

mechanisms across various catalytic fields.

Building on their previous work, Zhu et al. subsequently

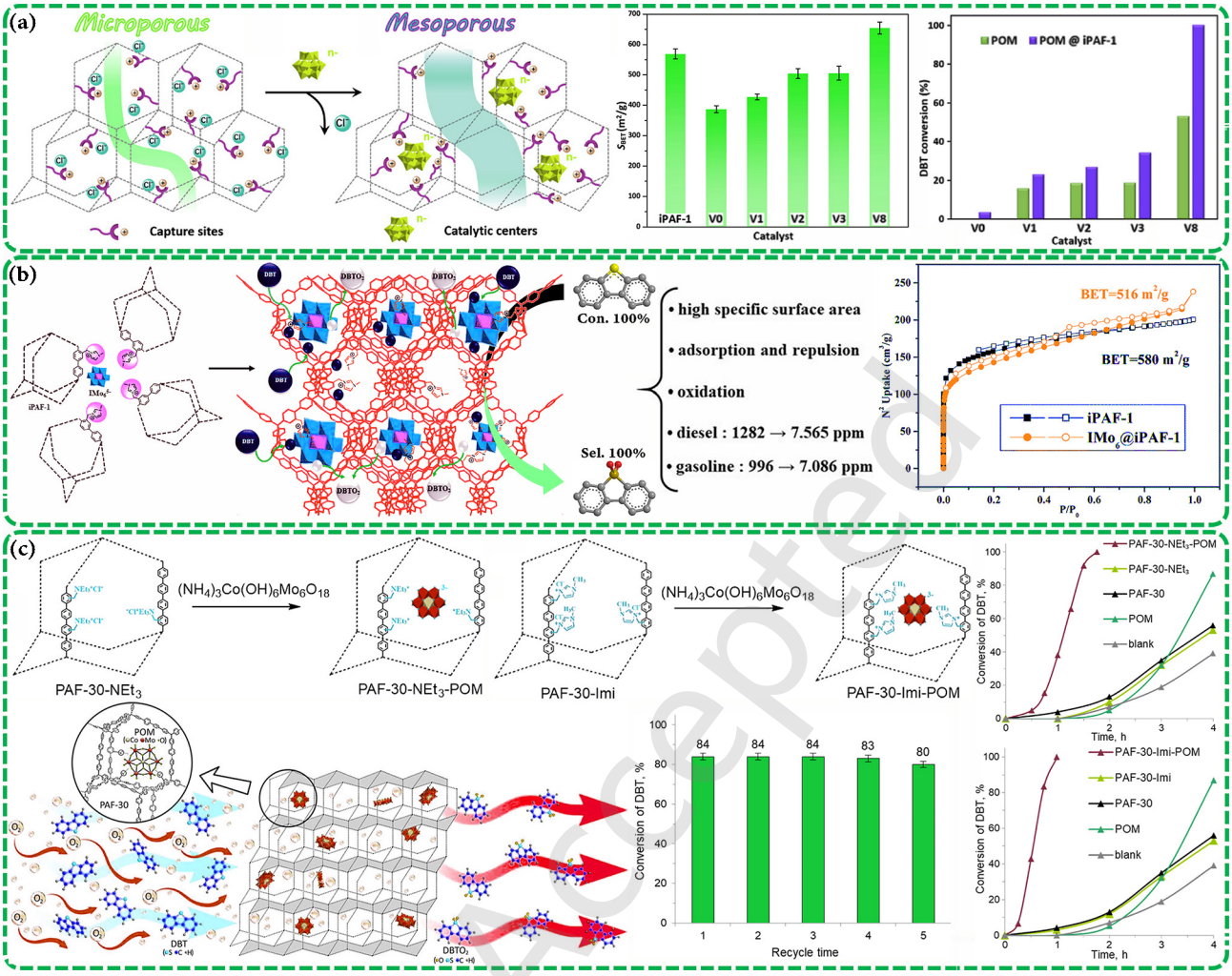

Figure 12 (a) Schematic synthetic route of **PMoV@iPAF-1**, BET surface area and catalytic DBT degradation performance of catalysts with different vanadium content. Reproduced with permission from Ref. [138], © Wiley-VCH GmbH. 2019. (b) Schematic synthetic route, isothermal adsorption desorption curve and catalytic performance of **IMo$_6$@iPAF-1**. Reproduced with permission from Ref. [56], © Royal Society of Chemistry 2020. (c) Schematic synthetic route, catalytic performance and cycle stability of **CoMo$_6$@iPAF-30**. Reproduced with permission from Ref. [140], © American Chemical Society 2023.

advanced a cationization modification strategy. By employing cationic PAFs (iPAF-1) which possess an inherent affinity for organic sulfur adsorption as capture platforms, they utilized Keggin-type $PMo_{12-n}V_n$ and Anderson-type $[IMo_6O_{24}]^{5-}$ (IMo_6) anions as active components. Through electrostatic self-assembly, they successfully fabricated a series of composite materials, namely **PMo$_{12-n}$V$_n$@iPAF-1** and **IMo$_6$@iPAF-1** [56, 138]. The fundamental innovation of this design is the bidirectional synergistic regulation between the capture and conversion units, effectively bypassing the performance limitations typical of conventional supported catalysts. Remarkably, the incorporation of POM active species does not lead to pore obstruction; instead, it triggers the formation of a hierarchical pore architecture that facilitates mass transfer. This structural evolution increases the specific surface area, thereby significantly boosting the frequency of contact between substrates and active sites (Fig. 12(a-b)). In aerobic ODS reactions, this catalytic system exhibits exceptional overall performance, achieving efficient desulfurization under mild conditions and maintaining high activity over seven consecutive cycles, which underscores its robust structural stability and reusability. Adopting a parallel strategy, the team also employs an imidazolium-functionalized ionic framework, iPAFs-270, to achieve a high loading capacity (up to 50%) of PMo_4V_8 and PW_{12} [139]. Performance evaluations reveal that **PMo$_4$V$_8$@iPAF-270** possesses remarkable activity in extractive ODS. Furthermore, owing to the inherent robustness of the PAF matrix, the material retained its structural integrity across a wide range of temperatures and pH levels, highlighting its considerable potential for industrial-scale applications.

Adopting the similar imidazolium functionalization approach discussed earlier, the research team led by Eseva performed surface ionization modifications on the hydrophobic porous aromatic framework PAF-30 (iPAF-30). This approach enabled the stable immobilization of Anderson-type $[CoMo_6O_{18}(OH)_6]^{3-}$ ($CoMo_6$) at the hydrophobic interface, successfully yielding a novel heterogeneous catalyst designated as **CoMo$_6$@iPAF-30** (Fig. 12(c)) [140]. Within an aerobic ODS system utilizing model oil, the researchers conduct a systematic investigation into how various factors, including the type of carrier functionalization, reaction

temperature, catalyst dosage, and the nature of sulfur-containing substrates, influence catalytic efficiency, ultimately identifying the optimal reaction parameters. Experimental results demonstrate that at 130 °C with an air flow rate of 6 L/h, **$CoMo_6$@iPAF-30** achieved complete (100%) conversion of DBT within just 60 min. Nevertheless, when compared to existing literature, the catalytic activity of this particular system is considered to be at a moderate or average level.

5. Conclusion and Outlook

5.1. Conclusion

This article systematically reviews and comprehensively summarizes the latest research advances and development trends in composite catalysts constructed by encapsulating POMs within emerging porous framework materials, namely MOFs and COFs, for the green oxidative transformation of sulfur-containing compounds. Addressing long-standing scientific challenges in practical applications of homogeneous POM catalysts, including tendencies toward agglomeration and leaching, insufficient exposure of active sites, and lack of substrate selectivity regulation, POM@MOFs and POM@COFs composites offer effective solutions through precise design and synergistic modulation of host-guest architectures. This review focuses on three representative application scenarios: selective oxidation of active sulfides in biomedicine, deep oxidative desulfurization of fuels in environmental and energy fields, and degradation of chemical warfare agent simulants in public safety. Synthesizing existing research findings, the superior catalytic performance of POM@MOFs and POM@COFs systems compared to individual components can be attributed to three key mechanisms.

(i) Dual effects of physical confinement and electrostatic anchoring. The unique periodic pore structures of MOFs and COFs provide nanoscale confined spaces that effectively inhibit agglomeration and leaching of POM nanoparticles. Simultaneously, strong electrostatic interactions between abundant functional groups on the framework surface and POMs ensure stable immobilization of active components, significantly enhancing catalyst recyclability and lifespan.

(ii) Host-guest electronic synergy. Efficient interfacial electron transfer between the host frameworks (MOFs/COFs) and POM active centers enables precise modulation of the electron cloud density and redox potential of POM metal centers. This optimizes catalytic reaction pathways, substantially improving intrinsic catalytic activity and reaction selectivity.

(iii) Fine-tuning of pore microenvironment. Atomic-level precision in adjusting pore size, channel geometry and surface hydrophilicity/hydrophobicity of porous frameworks not only achieves sieving effects for substrates of different sizes but also selectively enriches reactants and accelerates product desorption. This creates an ideal microreactor environment, further enhancing substrate specificity and reaction efficiency of the catalytic system.

5.2. Future Prospects and Challenges

Although the POMs@MOFs and POM@COFs composite catalytic systems have achieved a series of breakthrough advances in the green oxidation of sulfur-containing compounds and successfully addressed many inherent shortcomings of homogeneous POM catalysts, the transition from fundamental laboratory research to large-scale industrial application still faces multiple challenges, such as insufficient synthetic controllability, ambiguous structure-property relationships, limited mechanistic understanding, and poor engineering compatibility. Future studies may focus on the following five key dimensions to conduct systematic and forward-looking exploration and breakthroughs.

(i) Atomic-level precision innovation and green scalable upgrades in synthetic methodologies. Current mainstream methods, such as impregnation, ion exchange, and simple *in-situ* encapsulation strategies, commonly suffer from uneven POM loading, random distribution of active sites, weak host-guest interactions, and potential structural damage to POMs. One of the core future research directions lies in developing atomic-level precise construction techniques, for instance, *via* coordination-directed self-assembly, site-specific covalent bonding, or post-synthetic modification strategies, to precisely anchor POM units with specific composition and structure at predetermined nodes or within the channels of porous frameworks. This enables monodisperse, high-density, and oriented arrangement of active centers. Meanwhile, there is an urgent need to explore green, low-cost, and scalable synthesis processes, including mechanochemical ball milling, microwave-assisted rapid synthesis, continuous-flow synthesis, and scaled-up improvements of hydro-/solvo-thermal methods. These advancements will lay a practical foundation for industrial applications such as deep fuel desulfurization and large-scale industrial wastewater treatment.

(ii) Precise regulation achieves the optimal balance between porosity and active load. The encapsulation and immobilization of POMs occupy and compress the pore space of the carrier, leading to a decline in porosity, an increase in mass transfer resistance, and a reduction in substrate accessibility to active sites. Maintaining excellent pore structure and efficient mass transfer under high loading conditions is a core issue urgently needing breakthrough in this field.

Constructing a hierarchical pore architecture is an effective pathway to resolve this contradiction. Through the synergy of a micro-meso-macroporous multi-level system, where micropores/narrow mesopores confine POMs to inhibit agglomeration and leaching, and mesopores/macropores construct fast mass transfer channels to reduce diffusion resistance, it is possible to simultaneously enhance both active site loading and mass transfer efficiency. Future efforts require the development of precise and controllable synthesis techniques for hierarchical pores to achieve fine-tuning of pore size, distribution, and connectivity, thereby supporting the design and development of high-performance encapsulated catalysts.

Vacancy engineering is another core strategy to reconfigure the balance between loading and mass transfer, encompassing two main development directions: First, chemical anchoring mediated by structural vacancies. Traditional physical impregnation and electrostatic

adsorption struggle to control the spatial distribution of POMs, which is the root cause of random pore blockage. Future designs could involve carriers with well-defined vacancies (e.g., MOFs with coordinatively unsaturated sites, mesoporous materials with controllable defects), enabling the precise anchoring of POMs. This approach not only achieves spatial isolation and ordered arrangement of POMs, preventing agglomeration and pore blocking, but also suppresses leaching of active components through strong interactions. By matching vacancy density with loading amount, it holds promise for achieving single-cluster confinement, resolving the inherent conflict between loading and blockage at the molecular level. Second, on-demand pore channel regulation driven by dynamic vacancies. This involves constructing intelligent, reversible pore-blocking/release mechanisms.

(iii) Exploring structural diversity and precisely constructing structure-property relationships. The POM family possesses an extremely rich variety of structural types, ranging from classic Keggin, Wells-Dawson, and Lindqvist structures to various lacunary, substituted, sandwich-type, and chiral POMs. Their redox properties, acidity, and charge density can be finely tuned at the atomic scale. However, current studies have largely focused on only a few common POM structures, leaving a lack of systematic understanding of the intrinsic relationship between their structural diversity and catalytic performance. Future efforts should systematically investigate the structure-property relationships of different POM types, establishing quantitative structure-performance maps that correlate POM composition, topology, charge state with catalytic activity and selectivity. Building on this foundation, by precisely modulating the topology, pore size, and surface functional groups of porous frameworks, combined with electronic structure modification of POMs, it becomes possible to achieve precise recognition and highly selective conversion of substrates with varying steric and electronic effects, such as bulky aromatic sulfides and chiral sulfides. This will meet the stringent requirements for chemo-, regio-, and enantio-selectivity in fine chemical synthesis for biomedicine.

(iv) *In-situ* dynamic analysis of interfacial electron interactions and catalytic reaction mechanisms. Although the host-guest synergistic effect is widely recognized as the core mechanism behind the enhanced performance of POM@MOFs and POM@COFs systems, current understanding of its microscopic nature remains largely at the level of macroscopic phenomena description and theoretical speculation, lacking direct experimental evidence of dynamic evolution during reactions. Future research should shift its focus from static structural characterization toward the observation of dynamic processes. Advanced characterization techniques, such as in situ X-ray absorption fine structure, in situ Raman spectroscopy, quasi-in situ X-ray photoelectron spectroscopy, and in situ infrared spectroscopy, should be comprehensively employed to monitor in real time the valence state changes of POM active centers, the evolution of their coordination environments, and the charge transfer pathways at the host–guest interface. Furthermore, by integrating ultrafast spectroscopic techniques like femtosecond transient absorption spectroscopy, researchers can reveal how host-guest interactions modulate the energy barriers of reaction transition states, the stability of reaction intermediates, and the overall reaction pathways. This will provide a solid physicochemical foundation for the rational design of high-performance catalysts.

(v) Rational catalyst design driven by artificial intelligence (AI) and machine learning. With the continuous accumulation of experimental data and rapid advancements in computational chemistry within this field, the traditional trial-and-error approach to catalyst development can no longer meet the demands of efficient innovation. Introducing a paradigm for catalyst discovery driven by AI and machine learning has become an inevitable trend. Specifically, breakthroughs can be achieved through the following three aspects. Firstly, building machine learning models based on published experimental data and high-throughput DFT calculations to virtually screen a vast array of POM-porous frameworks combinations, enabling rapid prediction of their catalytic activity and selectivity in various sulfur oxidation reactions. Secondly, mining hidden correlations between the host-guest interfacial electronic structure, pore microenvironment, and catalytic performance to establish interpretable performance prediction models, which guide the directional synthesis of composite materials with specific catalytic functions. Thirdly, integrating AI with molecular dynamics simulations and reaction pathway calculations to deeply analyze the reaction kinetics and thermodynamics in POM-based heterogeneous catalytic systems, significantly shortening the research and development cycle from laboratory discovery to industrial application.

(vi) Long-term stability under harsh conditions and engineering application technology development. In real industrial application scenarios, catalysts must withstand complex and harsh chemical environments, such as high temperature, high pressure, high impurity content, and fluctuating pH, over extended periods. In emergency public safety events, such as chemical agent decontamination, they are also required to exhibit rapid response, high tolerance, and reusability. Most current studies only evaluate catalyst recyclability under ideal laboratory conditions, lacking in-depth investigation of their deactivation mechanisms (e.g., framework collapse, POM leaching, active site poisoning) under actual operating conditions. Future work should prioritize stability testing and deactivation mechanism studies under simulated industrial conditions, and develop porous framework materials with higher chemical stability, thermal stability, and anti-poisoning capability. In addition, to address engineering challenges associated with powdered catalysts, including difficult separation, easy loss, and high bed pressure drop, vigorously advancing monolithic catalyst fabrication techniques, such as supported thin-film catalysts, fibrous catalysts, and 3D-printed structured catalysts, will be a crucial step in advancing this technology from the laboratory to industrial application.

The cross-border integration of POMs and porous framework materials opens up a new research direction for the green oxidation conversion of sulfur-containing compounds and shows great application potential. In the

future, through the in-depth cross-collaboration of chemistry, materials science, environmental science, computational science and engineering science, combined with atomic-level precise synthesis strategies, *in-situ* dynamic mechanism exploration and AI-driven rational design, we will develop the next generation of efficient, stable, low-cost and environmentally friendly sulfur-containing oxidation catalytic systems, which will have far-reaching social impact and significant economic benefits in the fields of environmental remediation, pharmaceutical and chemical industry and public safety.

Data availability

All data necessary to support the findings of this study are included within the article. Further data associated with this work can be obtained from the corresponding author upon reasonable request.

Acknowledgements

This work was financially supported by the National Natural Science Foundation of China (No. 22401063, 22371066, 22071042, 22171070), the Talent Research Initiation Fund Project of Hainan Normal University (No. HSZK-KYQD-202407), the Scientific Research Support Project of Colleges and Universities in Hainan Province (No. Hnky2024-12), the Research Start-up Fund of Hainan University, China (No. KYQD(ZR)23039), the Open Fund of Key Laboratory of Electrochemical Energy Storage and Energy Conversion of Hainan Province (No. KFKT2024004), the Hainan Provincial Natural Science Foundation of China (No. 225QN219), and the Innovational Fund for Scientific and Technological Personnel of Hainan Province (No. KJRC2023D32), the Zhongyuan Talent Program Zhongyuan Leading Talents in Fundamental Research, the Key Project of the Youth Interdisciplinary Foundation of Henan University and the Program for Kaifeng Innovation Teams of Science and Technology.

Declaration of competing interest

The authors declare that they have no known competing financial interests or personal relationships that could have appeared to influence the work reported in this paper.

Author contribution statement

Y. H. Chen: Data curation, visualization, writing – original draft. S. Z. Chang: Data curation, visualization, resources, supervision, writing – review & editing. J. W. Zhao: resources, supervision, writing – review & editing. All the authors have approved the final.

Informed consent

Not applicable

Ethics statement

Not applicable

Use of AI statement

During the preparation of this work, the authors utilized Doubao, DeepSeek, and Yuanbao solely for the purpose of language polishing. After using these tools, the authors have reviewed and edited the content as necessary and take full responsibility for the content of the publication.

References

[1] Chang Y.; Zhou G.; Xu D.; Wang P.; Qin W.; Yan H. Enantioselective Organocatalytic Construction of Axially Chiral Sulfoxides. *Nat. Synth.*, **2025**, *4*, 1587–1597.

[2] Chen S. C.; Li X. M.; Battisti N.; Guan G.; Montoya M. A.; Osvatic J.; Pjevac P.; Pollak S.; Richter A., et al. Microbial Iron Oxide Respiration Coupled to Sulfide Oxidation. *Nature*, **2025**, *646*, 925-933.

[3] Li J.; Yang Z.; Li S.; Jin Q.; Zhao J. Review on Oxidative Desulfurization of Fuel by supported Heteropolyacid Catalysts. *J. Ind. Eng. Chem.*, **2020**, *82*, 1-16.

[4] Dong J.; Zhang D.; Zhang P.; Liu C.; Li J.; Bai J.; Chi Y.; Hu C. Polyoxometalates for the Decontamination of Chemical Warfare Agents: From Structure and Composition Regulation to Performance Enhancement. *Coord. Chem. Rev.*, **2024**, *517*, 215998.

[5] Gao A. P.; Zhao S. H.; Wang J. J.; Li H. L. State-of-the-Art of Polyoxometalate-Based Catalysts for Catalytic Removal of Vesicants. *Rev. Inorg. Chem.*, **2025**, 10.1515/revic-2025-0047.

[6] Chen Y.; Chang S.; Zhang J.; Wu Q.; Hua Y.; Pan Q. Recent Advances in Single-Crystal Polyoxometalate-Based Metal–Organic Complex Catalytic Systems for Sulfide–Sulfoxide Selective Transformations. *New J. Chem.*, **2026**, *50*, 5049-5075.

[7] Liu X.; Si C.; Xu J.; Sun H.; Li J.; Han Q. Constructing a Polyoxometalate-Based Metal-Organic Framework for Photocatalytic Oxidation of Thioethers to Sulfoxides Utilizing In Situ-Generated Superoxide Radicals. *Inorg. Chem.*, **2025**, *64*, 1263-1271.

[8] Xu Q.; Liang X.; Xu B.; Wang J.; He P.; Ma P.; Feng J.; Wang J.; Niu J. 36-Nuclearity Organophosphonate-Functionalized Polyoxomolybdates: Synthesis, Characterization and Selective Catalytic Oxidation of Sulfides. *Chem. Eur. J.*, **2020**, *26*, 14896-14902.

[9] Zhang Y.; Wang X.; Wang Y.; Xu N.; Wang X.-L. Anderson-Type Polyoxometalate-Based Sandwich Complexes Bearing a New "V"-Like Bis-Imidazole-Bis-Amide Ligand as Electrochemical Sensors and Catalysts for Sulfide Oxidation. *Polyoxometalates*, **2022**, *1*, 9140004.

[10] Yu L.; Liu R.; Li Y.; Wang R. Recent Advances and Challenges in Catalysts for Oxidative Desulfurization of Fuel Oils: A Review. *Energy Fuels*, **2025**, *39*, 19061-19092.

[11] Yang L.; Zhang Z.; Zhang C.-N.; Wang X.-L. A Bifunctional POM-Based Cu-Viologen Complex with Mixed Octamolybdate Clusters for Rapid Oxidation Desulfurization and Effective Photogeneration of Hydrogen. *Rare Met.*, **2023**, *43*, 236-246.

[12] Li J.; Zhang D.; Chi Y.; Hu C. Catalytic Application of Polyoxovanadates in the Selective Oxidation of Organic Molecules. *Polyoxometalates*, **2022**, *1*, 9140012.

[13] Kowalski P.; Mitka K.; Ossowska K.; Kolarska Z. Oxidation of Sulfides to Sulfoxides. Part 1: Oxidation Using Halogen Derivatives. *Tetrahedron*, **2005**, *61*, 1933-1953.

[14] Winterton N. *Chemistry for Sustainable Technologies: A Foundation*. The Royal Society of Chemistry, **2021**.

[15] Zimmerman J. B.; Anastas P. T.; Erythropel H. C.; Leitner W. Designing for a Green Chemistry Future. *Science*, **2020**, *367*, 397-400.

[16] Berzelius J. J. Beitrag zur näheren Kenntniss des Molybdäns. *Annalen der Physik*, **1826**, *82*, 369-392.

[17] Tang Z.; Li J.; Wang D.; Chen L.; Zhao J. Frontier Advances in Polyoxometalates Templated by Main Group VI Heteroatoms. *Coord. Chem. Rev.*, **2026**, *560*, 217880.

[18] Wei Y. Polyoxometalates: An Interdisciplinary Journal Focused on All Aspects of Polyoxometalates. *Polyoxometalates*, **2022**, *1*, 9140014.

[19] Dolbecq A.; Dumas E.; Mayer C. R.; Mialane P. Hybrid Organic-Inorganic Polyoxometalate Compounds: From Structural Diversity to

Applications. *Chem. Rev.*, **2010**, *110*, 6009-6048.

[20] Tang Z.; Tang M.; Wang D.; Chen L.; Zhao J. Research Progress in Trivalent Main Group V Heteroanion-Templated Polyoxometalates. *Coord. Chem. Rev.*, **2026**, *548*, 217156.

[21] Guan Y.; Xiao H.-P.; Li X.-X.; Zheng S.-T. Recent Advances on the Synthesis, Structure, and Properties of Polyoxotantalates. *Polyoxometalates*, **2023**, *2*, 9140023.

[22] Yang K.; Hu Y.; Zhang T.; Wang B.; Qin J.; Li N.; Zhao Z.; Zhao J.; Chao D. Triple-Functional Polyoxovanadate Cluster in Regulating Cathode, Anode, and Electrolyte for Tough Aqueous Zinc-Ion Battery. *Adv. Energy Mater.*, **2022**, *12*, 2202671.

[23] Du D. Y.; Qin J. S.; Li S. L.; Su Z. M.; Lan Y. Q. Recent Advances in Porous Polyoxometalate-Based Metal-Organic Framework Materials. *Chem. Soc. Rev.*, **2014**, *43*, 4615-4632.

[24] Wang S.-S.; Yang G.-Y. Recent Advances in Polyoxometalate-Catalyzed Reactions. *Chem. Rev.*, **2015**, *115*, 4893-4962.

[25] Chang S.; Chen Y.; Zhang J.; Pan Q.; Hua Y. Heterogeneous Polyoxometalate-Based Catalysts for Functionalized Quinones Synthesis: Systematic Advances, Prospects, and Challenges. *Chempluschem*, **2025**, *90*, e202500261.

[26] Li H.; Kong H.; Guo J.; Li B.; Zhang S.; Li S.; Zhao J.; Bai L. First Photocatalytic Synthesis of Cyclic Carbonates from CO_2 Using Bromide-Functionalized Polyoxometalate without Additional Cocatalyst. *ACS Sustainable Chem. Eng.*, **2024**, *12*, 16396-16408.

[27] Zang D.; Wang H. Polyoxometalate-Based Nanostructures for Electrocatalytic and Photocatalytic CO_2 Reduction. *Polyoxometalates*, **2022**, *1*, 9140006.

[28] Hu Q.; Zhou H.; Ding Y.; Wågberg T.; Han X. Advances in Bridging Homogeneous and Heterogeneous Water Oxidation Catalysis by Insolubilized Polyoxometalate Clusters. *ACS Catal.*, **2024**, *14*, 5898-5910.

[29] Zhou Y.; Chen G.; Long Z.; Wang J. Recent Advances in Polyoxometalate-Based Heterogeneous Catalytic Materials for Liquid-Phase Organic Transformations. *RSC Adv.*, **2014**, *4*, 42092-42113.

[30] Song N.; Lu M.; Liu J.; Lin M.; Shangguan P.; Wang J.; Shi B.; Zhao J. A Giant Heterometallic Polyoxometalate Nanocluster for Enhanced Brain-Targeted Glioma Therapy. *Angew. Chem., Int. Ed.*, **2024**, *63*, e202319700.

[31] Wang X.; Su Z., Polyoxometalate-Based Metal-Organic Frameworks. in Handbook of Metal-Organic Frameworks, eds. Bu X.-H.; Ma S., Springer Nature Singapore, Singapore, 2025, pp. 1-25.

[32] Li J.; Tang Z.; Chen L.; Zhao J. Recent Research Progress in Polyoxometalate-Based Composite Materials Applied to Electrochemical Biosensors for Biomolecule Detection. *Nanoscale*, **2025**, *17*, 21379-21399.

[33] Ebrahimi A.; Krivosudský L.; Khodabakhshi S.; Khaleghiabbasabadi M.; Sadeghi M.; Motola M. Polyoxometalate-Based Covalent Organic Frameworks: The Next Generation of Heterogeneous Catalysts. *Coord. Chem. Rev.*, **2026**, *548*, 217201.

[34] Li Y.; Yu J. Emerging Applications of Zeolites in Catalysis, Separation and Host-Guest Assembly. *Nat. Rev. Mater.*, **2021**, *6*, 1156-1174.

[35] Yue K.; Lu R.; Gao M.; Song F.; Dai Y.; Xia C.; Mei B.; Dong H.; Qi R., et al. Polyoxometalated Metal-Organic Framework Superstructure for Stable Water Oxidation. *Science*, **2025**, *388*, 430-436.

[36] Maru K.; Kalla S.; Jangir R. MOF/POM Hybrids as Catalysts for Organic Transformations. *Dalton Trans.*, **2022**, *51*, 11952-11986.

[37] Chang S.; Ruan B.; Zhang J.; Wu Q.; Pan Q. Recent Advances in Polyoxometalate@Porous-Framework Composite Catalysts for Oxidative Desulfurization. *Chem. Res. Chin. Univ.*, **2026**, 10.1007/s40242-026-6098-9.

[38] Lu M.; Zhang M.; Liu J.; Yu T. Y.; Chang J. N.; Shang L. J.; Li S. L.; Lan Y. Q. Confining and Highly Dispersing Single Polyoxometalate Clusters in Covalent Organic Frameworks by Covalent Linkages for CO_2 Photoreduction. *J. Am. Chem. Soc.*, **2022**, *144*, 1861-1871.

[39] Lei P.; Geng W.; Zhang H.; Zhang P.; Li J.; Du J.; Chi Y.; Hu C. Single-Cluster Polyoxometalate Catalysts via Modular Electrostatic Assembly on a Cationic Covalent Organic Framework for Furfural Electroreduction. *J. Mater. Chem. A*, **2026**, *14*, 8643-8653.

[40] Sun Z.; Wang R.; Kozhevnikov I. V. Versatile POMOF-Based Materials: Synthesis, Mechanism, Topology and Catalytic Applications. *Coord. Chem. Rev.*, **2025**, *524*, 216304.

[41] Kong S.; Zhang X.; Xu N.; Wang X. Recent Advances in Polyoxometalate-Covalent Organic Framework Composites: Rational Design, Structural Modulation, and Application Perspectives. *Dalton Trans.*, **2026**, *55*, 7429-7443.

[42] Zhang S.; Ou F.; Ning S.; Cheng P. Polyoxometalate-Based Metal-Organic Frameworks for Heterogeneous Catalysis. *Inorg. Chem. Front.*, **2021**, *8*, 1865-1899.

[43] Li C.; Zhang Y.; Shu L.; Teng Y.-L.; Wang Y.-R.; Dong B.-X. Boosting Electrochemical Reduction of CO_2 to CO via Fixation Keggin-Type Polyoxoanions $XW_{11}Co$ (X = Si, P, Co) into ZIF-8 Cavities: Pivotal Role of Central Atoms in Catalytic Performance. *Polyoxometalates*, **2025**, *4*, 9140097.

[44] Zhao H.-Y.; Li Y.-Z.; Zhao J.-W.; Wang L.; Yang G.-Y. State-of-the-Art Advances in the Structural Diversities and Catalytic Applications of Polyoxoniobate-Based Materials. *Coord. Chem. Rev.*, **2021**, *443*, 213966.

[45] Liu Y.; Tang C.; Cheng M.; Chen M.; Chen S.; Lei L.; Chen Y.; Yi H.; Fu Y., et al. Polyoxometalate@Metal–Organic Framework Composites as Effective Photocatalysts. *ACS Catal.*, **2021**, *11*, 13374-13396.

[46] Liu J. C.; Han Q.; Chen L. J.; Zhao J. W.; Streb C.; Song Y. F. Aggregation of Giant Cerium-Bismuth Tungstate Clusters into a 3D Porous Framework with High Proton Conductivity. *Angew. Chem., Int. Ed.*, **2018**, *57*, 8416-8420.

[47] Palermo V.; Martinez J. J.; Romanelli G. P. Recent Contributions on Heteropoly Compounds as Suitable Catalysts in Selective Oxidation of Organic Substrates. *Curr. Org. Chem.*, **2023**, *27*, 1230-1254.

[48] Liu X. B.; Rong Q.; Tan J.; Chen C.; Hu Y. L. Recent Advances in Catalytic Oxidation of Organic Sulfides: Applications of Metal–Ionic Liquid Catalytic Systems. *Frontiers in Chemistry*, **2022**, *9*, 798603.

[49] Yang J.; Gao M.; Zhang M.; Zhang Y.; Gao M.; Wang Z.; Xu L.; Wang X.; Shen B. Advances in the Adsorption and Degradation of Chemical Warfare Agents and Simulants by Metal-Organic Frameworks. *Coord. Chem. Rev.*, **2023**, *493*, 215289.

[50] Zhang Y.; Liu Y.; Wang D.; Liu J.; Zhao J.; Chen L. State-of-the-Art Advances in the Syntheses, Structures, and Applications of Polyoxometalate-Based Metal–Organic Frameworks. *Polyoxometalates*, **2023**, *2*, 9140017.

[51] Ding X.-X.; Yuan Y.-Y.; Zhang Y.-G.; Jiang Z.-G.; Zhan C.-H. Chiral Polyoxometalate–Cyclodextrin Frameworks via Mn-Mediated Assembly: Enhanced Stability and Catalytic Activity. *Polyoxometalates*, **2024**, *3*, 9140046.

[52] Liu G.; Jiang J.; Zeng B.; Li Y.; Chen L.; Zhao J. Core–Shell Heterostructured Composite Architected from a Multilanthanide-Included Phospho(III)tungstate and MIL-(53)Fe as a Nanozyme for Catalytic Oxidation of 3,3′,5,5′-Tetramethylbenzidine. *Inorg. Chem.*, **2026**, *65*, 3626-3637.

[53] Huang J.; Liu J.; Tian L.; Li X.; Ma X.; Yu X.; Guo Q.; Zhao J. Ultrathin Carbon-Coated Zr^{3+}-ZrO_2 Nanostructures for Efficient Visible Light Photocatalytic Antibiotic Elimination. *Chem. Eng. J.*, **2021**, *412*, 128621.

[54] Samaniyan M.; Mirzaei M.; Khajavian R.; Eshtiagh-Hosseini H.; Streb C. Heterogeneous Catalysis by Polyoxometalates in Metal–Organic Frameworks. *ACS Catal.*, **2019**, *9*, 10174-10191.

[55] Buru C. T.; Farha O. K. Strategies for Incorporating Catalytically Active Polyoxometalates in Metal–Organic Frameworks for Organic Transformations. *ACS Appl. Mater. Interfaces*, **2020**, *12*, 5345-5360.

[56] Li Y.; Song J.; Jiang M.; Bawa M.; Wang X.; Tian Y.; Zhu G. The Fabrication of IMo_6@iPAF-1 as an Enzyme Mimic in Heterogeneous Catalysis for oxidative Desulfurization under O_2 or Air. *J. Mater. Chem. A*, **2020**, *8*, 9813-9824.

[57] Sun J.-Y.; Sun S.-Y.; Zhang Z.; Li M.-T.; Liu G.-C.; Wang X.-L. A 4,4-Connected 2D POM-Based Complex with Synergistic Mixed-Valence Cu^{I}/Cu^{II} for Mild and Efficient Catalytic Oxidation of Phenols. *J. Mater. Chem. A*, **2026**, *14*, 15000-15007.

[58] Geng K.; He T.; Liu R.; Dalapati S.; Tan K. T.; Li Z.; Tao S.; Gong Y.; Jiang Q., et al. Covalent Organic Frameworks: Design, Synthesis, and Functions. *Chem. Rev.*, **2020**, *120*, 8814-8933.

[59] Tian Y.; Zhu G. Porous Aromatic Frameworks (PAFs). *Chem. Rev.*,

2020, *120*, 8934-8986.

[60] Tan K. T.; Ghosh S.; Wang Z.; Wen F.; Rodríguez-San-Miguel D.; Feng J.; Huang N.; Wang W.; Zamora F., et al. Covalent organic frameworks. *Nature Reviews Methods Primers*, **2023**, *3*, 1.

[61] Cote A. P.; Benin A. I.; Ockwig N. W.; O'Keeffe M.; Matzger A. J.; Yaghi O. M. Porous, Crystalline, Covalent Organic Frameworks. *Science*, **2005**, *310*, 1166-1170.

[62] Ge S.; Wei K.; Peng W.; Huang R.; Akinlabi E.; Xia H.; Shahzad M. W.; Zhang X.; Xu B. B., et al. A Comprehensive Review of Covalent Organic Frameworks (COFs) and Their Derivatives in Environmental Pollution Control. *Chem. Soc. Rev.*, **2024**, *53*, 11259-11302.

[63] Pakulski D.; Gorczyński A.; Brykczyńska D.; Montes-García V.; Czepa W.; Janica I.; Bielejewski M.; Kubicki M.; Patroniak V., et al. New Anderson-Based Polyoxometalate Covalent Organic Frameworks as Electrodes for Energy Storage Boosted Through Keto-Enol Tautomerization. *Angew. Chem., Int. Ed.*, **2023**, *62*, 202305239.

[64] Dai X.; Zhang Y.; Zhao Y.; Li S.; Ma N.; Xia Q.; Liu Y.; Liu R.; Liu S., et al. Polarity-Directed Synthesis of an Exfoliable 2D Polyoxometalate-Based Metal-Organic Framework for Noble Metal-Free Alkyne Transfer Semi-Hydrogenation. *Angew. Chem., Int. Ed.*, **2026**, 10.1002/anie.7007153.

[65] Chen L.; Chen W.-L.; Wang X.-L.; Li Y.-G.; Su Z.-M.; Wang E.-B. Polyoxometalates in Dye-Sensitized Solar Cells. *Chem. Soc. Rev.*, **2019**, *48*, 260-284.

[66] Zhang H.; Wang B.; Yu X.; Li J.; Shang J.; Yu J. Carbon Dots in Porous Materials: Host-Guest Synergy for Enhanced Performance. *Angew. Chem., Int. Ed.*, **2020**, *59*, 19390-19402.

[67] An Y.; Wang L.; Jiang W.; Lv X.; Yuan G.; Hang X.; Pang H. Metal-Organic Framework-Based Materials for Photocatalytic Overall Water Splitting: Status and Prospects. *Polyoxometalates*, **2023**, *2*, 9140030.

[68] Li J.; Wu D.; Cheng Z.; Wu H.; Hua Y.; Chen H. Iron-Induced Structural Modulation of Nickel and Iron Layered Double Hydroxides Cathodes for Aqueous Zinc-Ion Batteries. *Prog. Solid State Chem.*, **2026**, *83*, 100589.

[69] Haruna A.; Merican Z. M. A.; Rahman M. B. A.; Musa S. G.; Al-Yaari A. Fabrication of $PW_{11}Zn$@MOF-808 and Its Catalytic Activity for Oxidative Desulfurization of Fuel Oil: Kinetics, Thermodynamics and Mechanism. *J. Solid State Chem.*, **2023**, *326*, 124232.

[70] Silva D. F.; Faria R. G.; Santos-Vieira I.; Cunha-Silva L.; Granadeiro C. M.; Balula S. S. Simultaneous Sulfur and Nitrogen Removal from Fuel Combining Activated Porous MIL-100(Fe) Catalyst and Sustainable Solvents. *Catal. Today*, **2023**, *423*, 114250.

[71] Banerjee R.; Phan A.; Wang B.; Knobler C.; Furukawa H.; O'Keeffe M.; Yaghi O. M. High-Throughput Synthesis of Zeolitic Imidazolate Frameworks and Application to CO_2 Capture. *Science*, **2008**, *319*, 939-943.

[72] Buru C. T.; Li P.; Mehdi B. L.; Dohnalkova A.; Platero-Prats A. E.; Browning N. D.; Chapman K. W.; Hupp J. T.; Farha O. K. Adsorption of a Catalytically Accessible Polyoxometalate in a Mesoporous Channel-type Metal-Organic Framework. *Chem. Mater.*, **2017**, *29*, 5174-5181.

[73] Férey G.; Mellot-Draznieks C.; Serre C.; Millange F.; Dutour J.; Surblé S.; Margiolaki I. A Chromium Terephthalate-Based Solid with Unusually Large Pore Volumes and Surface Area. *Science*, **2005**, *309*, 2040-2042.

[74] Chang X.; Yang X. F.; Qiao Y.; Wang S.; Zhang M. H.; Xu J.; Wang D. H.; Bu X. H. Confined Heteropoly Blues in Defected Zr-MOF (Bottle Around Ship) for High-Efficiency Oxidative Desulfurization. *Small*, **2020**, *16*, e1906432.

[75] Zhang R.; Ding H.; Pu X.; Qian Z.; Xiao Y. Recent Advances in the Synthesis of Sulfides, Sulfoxides and Sulfones via C-S Bond Construction from Non-Halide Substrates. *Catalysts*, **2020**, *10*, 1339.

[76] Hoque M. A.; Jiang T.; Poole D. L.; Stahl S. S. Manganese-Mediated Electrochemical Oxidation of Thioethers to Sulfoxides Using Water as the Source of Oxygen Atoms. *J. Am. Chem. Soc.*, **2024**, *146*, 21960-21967.

[77] Wang S.; Tang L.; Cai B.; Yin Z.; Li Y.; Xiong L.; Kang X.; Xuan J.; Pei Y., et al. Ligand Modification of Au_{25} Nanoclusters for Near-Infrared Photocatalytic Oxidative Functionalization. *J. Am. Chem. Soc.*, **2022**, *144*, 3787-3792.

[78] Zhao X.; Duan Y.; Yang F.; Wei W.; Xu Y.; Hu C. Efficient Mechanochemical Synthesis of Polyoxometalate⊂ZIF Complexes as Reusable Catalysts for Highly Selective Oxidation. *Inorg. Chem.*, **2017**, *56*, 14506-14512.

[79] Bai X.; Han X.; Wang Y.; Zhang A.; Yang Y.; Lu Y.; Liu S. Two 3D Two-Fold Interpenetrated Dia-Like Polyoxometalate-Based Metal-Organic Frameworks: Synthesis and Sulfide Selective Oxidation Activity. *Inorg. Chem.*, **2023**, *62*, 13221-13229.

[80] Wang J.; Liu Y.; Yuan Z.; Li L.; Ma P.; Wang J.; Niu J. Visible-Light-Responsive Polyoxometalate@Metal-Organic Frameworks Involving Ir Metalloligands for Highly Selective Photocatalytic Oxidation of Sulfides to Sulfoxide. *Chem. Eur. J.*, **2023**, *30*, e202303401.

[81] Buru C. T.; Lyu J.; Liu J.; Farha O. K. Restricting Polyoxometalate Movement Within Metal-Organic Frameworks to Assess the Role of Residual Water in Catalytic Thioether Oxidation Using These Dynamic Composites. *Front. Mater.*, **2019**, *6*, 152.

[82] Buru C. T.; Platero-Prats A. E.; Chica D. G.; Kanatzidis M. G.; Chapman K. W.; Farha O. K. Thermally Induced Migration of a Polyoxometalate within a Metal-Organic Framework and Its Catalytic Effects. *J. Mater. Chem. A*, **2018**, *6*, 7389-7394.

[83] Buru C. T.; Wasson M. C.; Farha O. K. $H_5PV_2Mo_{10}O_{40}$ Polyoxometalate Encapsulated in NU-1000 Metal-Organic Framework for Aerobic Oxidation of a Mustard Gas Simulant. *ACS Appl. Nano Mater.*, **2019**, *3*, 658-664.

[84] Sun Z.-B.; Wang Q.-Y.; Li C.; Cao M.; Zhang J.-Z.; Wu J. Atomically Synergistic Bimetallic Pair Sites in a Dual-Cluster-Based MOF for Ultrafast Degradation of Chemical Warfare Agent Simulants. *Nano Res.*, **2025**, *18*, 94907196.

[85] Li Y.; Gao Q.; Zhang L.; Zhou Y.; Zhong Y.; Ying Y.; Zhang M.; Huang C.; Wang Y. $H_5PV_2Mo_{10}O_{40}$ Encapsulated in MIL-101(Cr): Facile Synthesis and Characterization of Rationally Designed Composite Materials for Efficient Decontamination of Sulfur Mustard. *Dalton Trans.*, **2018**, *47*, 6394-6403.

[86] Zhai Y.; Yu J.; Zhang L.; Zhou Y.; Zhong Y.; Yang Y.; Wang Y. A. A Bifunctional Composite $H_5PV_2Mo_{10}O_{40}$@MOF-808(Ce): Preparation, Characterization, and Performance in the Decontamination of Chemical Warfare Agent Surrogates CEES and DMNP. *Microporous Mesoporous Mater.*, **2021**, *322*, 111163.

[87] Wang J.; Huo H.; Wang Y.; Zhang Z.; Liu S. General Strategy for In situ Synthesis of NENU-n Series Polyoxometalate-based MOFs on Copper Foil. *Chem. J. Chin. Universities*, **2022**, *43*, 20210557.

[88] Granadeiro C. M.; Barbosa A. D. S.; Ribeiro S.; Santos I. C. M. S.; de Castro B.; Cunha-Silva L.; Balula S. S. Oxidative Catalytic Versatility of a Trivacant Polyoxotungstate Incorporated into MIL-101(Cr). *Catal. Sci. Technol.*, **2014**, *4*, 1416-1425.

[89] Gao Y.; Granadeiro C. M.; Cunha-Silva L.; Zhao J.; Balula S. S. Peroxomolybdate@MOFs as Effective Catalysts for Oxidative Desulfurization of Fuels: Correlation between MOF Structure and Catalytic Activity. *Catal. Sci. Technol.*, **2023**, *13*, 4785-4801.

[90] Julião D.; Gomes A. C.; Pillinger M.; Valença R.; Ribeiro J. C.; de Castro B.; Gonçalves I. S.; Cunha Silva L.; Balula S. S. Zinc-Substituted Polyoxotungstate@Amino-MIL-101(Al) – An Efficient Catalyst for the Sustainable Desulfurization of Model and Real Diesels. *Eur. J. Inorg. Chem.*, **2016**, *2016*, 5114-5122.

[91] Granadeiro C. M.; Nogueira L. S.; Julião D.; Mirante F.; Ananias D.; Balula S. S.; Cunha-Silva L. Influence of a Porous MOF Support on the Catalytic Performance of Eu-Polyoxometalate Based Materials: Desulfurization of a Model Diesel. *Catal. Sci. Technol.*, **2016**, *6*, 1515-1522.

[92] Sun M.; Chen W.-C.; Zhao L.; Wang X.-L.; Su Z.-M. A PTA@MIL-101(Cr)-Diatomite Composite as Catalyst for Efficient Oxidative Desulfurization. *Inorg. Chem. Commun.*, **2018**, *87*, 30-35.

[93] Gao Y.; Yan M.; Dong X.; Jia H.; Zhao X.; He Y.; Guo L.; Zhao J. Boosting Extraction Oxidation Desulfurization via Valence Modulation: $(TBA)_3PMo^{V}_4$@MOF-808(Zr) Outperforms Its Hexavalent Analog. *Fuel*, **2026**, *406*, 137089.

[94] Gao Y.; Zhao S.; Huang J.; Han T.; Zhao J. A Size-Matched Composite

$(CTA)_3PW_4$@UiO-67 for the Ultra-Deep Desulfurization of Simulated Diesel: Design, Performance, and Reusability. *Appl. Organomet. Chem.*, **2024**, *39*, e7774.

[95] Ye G.; Zheng M.; Zhang Q.; Zhou J.; Wu L.; Wang J. Defect-Mediated Synergistic Effect of POM/UiO-66(Zr) Host-Guest Catalysts for Robust Deep Desulfurization at Ambient Temperature. *Small*, **2023**, *19*, 2301035.

[96] Fakhri H.; Firooz M. H.; Moteallemi A.; Esrafili A.; Yeganeh M.; Pasalari H.; Farzadkia M. Development and Optimization of Polyoxometalate-Modified Metal-Organic Frameworks for Efficient Removal of Sulfur and Nitrogen Compounds from Diesel Fuel under Visible Light. *Sci. Rep.*, **2026**, *16*, 4263.

[97] Wei P.; Yang Y.; Li W.; Li G. Keggin-POM@rht-MOF-1 Composite as Heterogeneous Catalysts towards Ultra-Deep Oxidative Fuel Desulfurization. *Fuel*, **2020**, *274*, 117834.

[98] Bai Y.; Xin Y.; Liu J.; Ma L.; Li G. Construction of $H_6PW_9V_3O_{40}$@rht-MOF-1 for Deep Oxidative Desulfurization of Fuel Oil. *Appl. Organomet. Chem.*, **2022**, *36*, e6633.

[99] Gao Y.; Lv Z.; Gao R.; Zhang G.; Zheng Y.; Zhao J. Oxidative Desulfurization Process of Model Fuel under Molecular Oxygen by Polyoxometalate Loaded in Hybrid Material CNTs@MOF-199 as Catalyst. *J. Hazard. Mater.*, **2018**, *359*, 258-265.

[100] Devendar P.; Yang G. F. Sulfur-Containing Agrochemicals. *Top. Curr. Chem.*, **2017**, *375*, 82.

[101] Benedetto Tiz D.; Rosati O.; Sancineto L. Sulfur- and Phosphorus-Containing FDA Approved Drugs in the Last Five Years (2020–2024): A Journey Among Small Molecules. *Phosphorus, Sulfur, and Silicon and the Related Elements*, **2025**, *200*, 1-39.

[102] Sun J.-Y.; Wang Z.-L.; Zhang Z.; Liu G.-C.; Wang X.-L. Hydrothermal Synthesis, Structure, and Catalytic Properties of a (4,6)-Connected Framework Constructed from Keggin-Type Polyoxometalate Units and Tetranuclear Copper Complexes. *Polyoxometalates*, **2024**, *3*, 9140039.

[103] Smirnova O.; Hwang S.; Sajzew R.; Ge L.; Reupert A.; Nozari V.; Savani S.; Chmelik C.; Reithofer M. R., et al. Precise Control Over Gas-Transporting Channels in Zeolitic Imidazolate Framework Glasses. *Nat. Mater.*, **2024**, *23*, 262-270.

[104] Park K. S.; Ni Z.; Cote A. P.; Choi J. Y.; Huang R.; Uribe-Romo F. J.; Chae H. K.; O'Keeffe M.; Yaghi O. M. Exceptional Chemical and Thermal Stability of Zeolitic Imidazolate Frameworks. *PNAS*, **2006**, *103*, 10186-10191.

[105] Cabanero D. C.; Rovis T. Low-Energy Photoredox Catalysis. *Nat. Rev. Chem.*, **2024**, *9*, 28-45.

[106] Kumar N.; Patial B.; Navdeep; Gupta R.; Bansal A. From Framework to Function: MOF-Derived Nanoparticles in Photocatalysis, Electrocatalysis, Adsorption, and Energy Storage. *Coord. Chem. Rev.*, **2026**, *550*, 217391.

[107] Liu R.; Zhao D.; Ji S.; Shao H.; Chen Y.; Feng M.; Wang T.; Li J.; Lin M., et al. Harvesting Singlet and Triplet Excitation Energies in Covalent Organic Frameworks for Highly Efficient Photocatalysis. *Nat. Mater.*, **2025**, *24*, 1245-1257.

[108] Wang S.; Dai Y.; Zhang J.; Tong Y.; Yang J.; Liu S.; Dai Z.; Meng X. Construction of Functional Metal-Organic Frameworks and Their Applications in the Biomedical Field. *Chem. Res. Chin. Univ.*, **2026**, *42*, 63-83.

[109] Guo S.; Pan C. W.; Hou M.; Hou Y. T.; Yao S.; Lu T. B.; Zhang Z. M. Dual Regulation of Sensitizers and Cluster Catalysts in Metal-Organic Frameworks to Boost H_2 Evolution. *Angew. Chem., Int. Ed.*, **2024**, *64*, e202420398.

[110] Kong X. J.; Lin Z.; Zhang Z. M.; Zhang T.; Lin W. Hierarchical Integration of Photosensitizing Metal-Organic Frameworks and Nickel-Containing Polyoxometalates for Efficient Visible-Light-Driven Hydrogen Evolution. *Angew. Chem., Int. Ed.*, **2016**, *55*, 6411-6416.

[111] Chauhan S.; Chauhan S.; D'Cruz R.; Faruqi S.; Singh K. K.; Varma S.; Singh M.; Karthik V. Chemical Warfare Agents. *Environ. Toxicol. Pharmacol.*, **2008**, *26*, 113-122.

[112] Hu X.; Cao M.; Zhang X.; Guo J.; Zhong Y.; Wu J.; Hou H.; Zang S. Bioinspired Hierarchical Zr-MOFs with Alkaline-Grafted Active Sites for Solid-Phase Hydrolysis of Nerve Agent Simulants. *Nano Res.*, **2026**, 10.26599/nr.2026.94908688.

[113] Li S.; Zheng Y.; Liu G.-C.; Li X.-H.; Zhang Z.; Wang X.-L. New Two Fold Interpenetrating 3D Polyoxovanadate-Based Metal-Organic Framework as Bifunctional Catalyst for the Removal of 2-Chloroethyl Ethyl Sulfide and Phenolic Compounds. *Polyoxometalates*, **2024**, *3*, 9140061.

[114] Kumar V.; Anslyn E. V. A Selective Turn-On Fluorescent Sensor for Sulfur Mustard Simulants. *J. Am. Chem. Soc.*, **2013**, *135*, 6338-6344.

[115] Li B.; Li S.; Wang B.; Meng Z.; Wang Y.; Meng Q.; Li C. Capture of Sulfur Mustard by Pillar[5]arene: From Host-Guest Complexation to Efficient Adsorption Using Nonporous Adaptive Crystals. *iScience*, **2020**, *23*, 101443.

[116] Jabbour C. R.; Parker L. A.; Hutter E. M.; Weckhuysen B. M. Chemical Targets to Deactivate Biological and Chemical Toxins Using Surfaces and Fabrics. *Nat. Rev. Chem.*, **2021**, *5*, 370-387.

[117] Tang M. J.; Arriaga Gomez J. C.; Manriquez D.; Yao X.; Hao Y.; Chen H.; Li Y.; An L.; Qi L., et al. Photooxidation of Organic Sulfide Enhanced by Heavy Atom Effect in Porphyrin Metal-Organic Frameworks with a Sea Topology. *ACS Catal.*, **2026**, *16*, 5004-5013.

[118] Liu Y.; Howarth A. J.; Hupp J. T.; Farha O. K. Selective Photooxidation of a Mustard-Gas Simulant Catalyzed by a Porphyrinic Metal-Organic Framework. *Angew. Chem., Int. Ed.*, **2015**, *54*, 9001-9005.

[119] Cheng Z.; Fahy K. M.; Peterson G. W.; Kirlikovali K. O.; Farha O. K. Advancing Metal-Organic Framework-Based Composites for Effective Chemical Warfare Agent Detoxification under Real-World Conditions. *Adv. Mater.*, **2025**, *37*, 2413848.

[120] Sun C.-Y.; Liu S.-X.; Liang D.-D.; Shao K.-Z.; Ren Y.-H.; Su Z.-M. Highly Stable Crystalline Catalysts Based on a Microporous Metal-Organic Framework and Polyoxometalates. *J. Am. Chem. Soc.*, **2009**, *131*, 1883-1888.

[121] Zhang H.; Wu C.; Zhang H.; Wang N.; Song Y.; Han L.; Zhang S.; Su M.; Liu J., et al. Hydrodesulfurization Catalysts for Ultra-Clean Diesel: Recent Progress, Modulation Strategies, and Emerging Alternatives. *Fuel*, **2026**, *417*, 138542.

[122] Sun F.; Ju Y.; Bao W.; Xu C.; Di H.; Meng X.; Wang S.; Yue C.; Zhao Y., et al. Dynamic Hydrogen Management System: Atomic-Level AlO Site *In Situ* Construction of Brønsted Acid Optimizes Co_3S_4@AlO-CoMoS Hydrogen Spillover for Low-Temperature Hydrogenation Reaction. *ACS Catal.*, **2026**, *16*, 9024–9043.

[123] Wu P.; Ma S.; Zhu W. Green Pathways to Low-Sulfur Diesel: Advances and Challenges in Desulfurization Technologies. *Green Chem.*, **2026**, *28*, 37-95.

[124] Rajendran A.; Cui T.-Y.; Fan H.-X.; Yang Z.-F.; Feng J.; Li W.-Y. A Comprehensive Review on Oxidative Desulfurization Catalysts Targeting Clean Energy and Environment. *J. Mater. Chem. A*, **2020**, *8*, 2246−2285.

[125] Tian X.; Huang S.; Tang Y.; Feng H.; Liu L.; Liu H.; Wang J. Tuning the Oxygen Vacancy Formation Energy of Ceria by Doping First Row Transition Metals for Aerobic Oxidation Desulfurization. *Chem. Commun.*, **2026**, *62*, 8466-8470.

[126] Wu J.; Zhang Y.; Yang C.; Feng J.; Fu S.; Ma T.; Liu J.; Wang C.; Zhen Y., et al. Oxidative Desulfurization Coupled with Nitrate Reduction Enables Energy-Efficient Operation at Ampere-Level Current Densities in an Anion Exchange Membrane Electrolyzer. *Appl. Catal. B Environ*, **2026**, *394*, 126868.

[127] Taghizadeh M.; Mehrvarz E.; Taghipour A. Polyoxometalate as an Effective Catalyst for the Oxidative Desulfurization of Liquid Fuels: A Critical Review. *Rev. Chem. Eng.*, **2020**, *36*, 831-858.

[128] Yan M.; Dong X.; Zhao J.; Gao Y. Engineering MOF-808 Composites with Peroxo-Polyoxometalates: Impregnation vs. Solvothermal Synthesis for Optimal Catalytic Oxidative Desulfurization. *J. Sulfur Chem.*, **2026**, *47*, 223-240.

[129] Gelogo A. C. G.; Choi A. E. S.; Dugos N. P.; Wan M. W. J. C. E. T. Catalyst Support Strategies: Encapsulation of Polyoxometalate Catalysts in Magnetic Particles in Oxidative Desulphurization. *Chem. Eng. Trans.*, **2025**, *122*, 43-48.

[130] Guo Y.; Liu X.; Liu X.; Xu N.; Wang X. A Series of Polyoxometalate-Based COF Composites by One-Pot Mechanosynthesis of Thioether to Sulfone. *Dalton Trans.*, **2023**, *52*, 12264-12270.

[131] Chen J.; Wang J.; Liu X.; Xu N.; Li H.; Wang X. Ultrasonic-Assisted Catalytic Oxidation of Sulfide: A Highly Efficient Keggin-POM@RT-COF-1 Catalvst Activated by Sonoluminescence. *Inorg. Chem. Commun.*, **2026**, *190*,

116937.

[132] Zhu Q.; An H.; Xu T.-Q.; Chen Y.; Wei Y.; Sun H. Polyoxometalates Embedded into Covalent Triazine Frameworks Regulating Charge Transfer for Visible-Light-Driven Synthesis of Functionalized Sulfoxides and Detoxification of Mustard Gas Simulants. *ACS Sustainable Chem. Eng.*, **2024**, *12*, 1655-1665.

[133] Zhu Q.; An H.; Xu T.; Chang S.; Chen Y.; Luo H.; Huang Y. PW_{12}-M@COFs as Efficient Photocatalysts for Visible-Light-Driven Oxidation of Various Sulfides and Degradation of Chemical Warfare Agent Simulant. *Appl. Catal., A*, **2023**, *662*, 119283.

[134] Zhu Q.; An H.; Wei Y.; Sun H.; Fu J.; Xu T.-Q. Confining Polyoxometalates in Porphyrin-Based Porous Cationic Polymer toward Boosting Visible-Light-Driven Synthesis of Sulfoxides and Detoxification of Mustard Gas Simulants. *J. Catal.*, **2024**, *436*, 115627.

[135] Zhu Q.; An H.; Fu J.; Sun H.; Zhang Y.; Xu T.-Q. Dawson-Type Polyoxometalates Functionalized Porphyrin-Based Covalent Organic Frameworks for Visible-Light-Driven Oxidation of Sulfides and Detoxification of Mustard Gas Simulants. *Inorg. Chem.*, **2025**, *64*, 16223−16233.

[136] Wang P.; Jiang L.; Zou X.; Tan H.; Zhang P.; Li J.; Liu B.; Zhu G. Confining Polyoxometalate Clusters into Porous Aromatic Framework Materials for Catalytic Desulfurization of Dibenzothiophene. *ACS Appl. Mater. Interfaces*, **2020**, *12*, 25910-25919.

[137] Lin Y.; Zhao X.; Chang S.; Zhang Y.; Gan L.; Tian Y.; Pan Q.; Zhu G. Enhancing Oxidative Desulfurization of Polyoxometalate by Integrating with a Self-Reductive Framework. *Sci. China Mater.*, **2024**, *67*, 2925−2933.

[138] Song J.; Li Y.; Cao P.; Jing X.; Faheem M.; Matsuo Y.; Zhu Y.; Tian Y.; Wang X., et al. Synergic Catalysts of Polyoxometalate@Cationic Porous Aromatic Frameworks: Reciprocal Modulation of Both Capture and Conversion Materials. *Adv. Mater.*, **2019**, *31*, e1902444.

[139] Zhang Z.; Zhai Y.; Gu M.; Lei H.; Li Y.; Li Y.; Tian Y.; Zhu G. Ionic Porous Aromatic Frameworks Embedding Polyoxometalates for Heterogeneous Catalysis. *Chem. Eur. J.*, **2024**, *30*, e202400796.

[140] Eseva E. A.; Lukashov M. O.; Kulikov L. A.; Grafov O. Y.; Bikbaeva A. F.; Akopyan A. V. Transition to Carbon Materials: The Effect of Support Nature on the Catalytic Properties of Anderson-Type Polyoxometalate in Aerobic Oxidation of Sulfur-Containing Compounds. *Energy Fuels*, **2023**, *37*, 17461-17472.

[141] Mishra B.; Alam A.; Chakraborty A.; Kumbhakar B.; Ghosh S.; Pachfule P.; Thomas A. Covalent Organic Frameworks for Photocatalysis. *Adv. Mater.*, **2025**, *37*, e2413118.

[142] Sun H.; Wu M.; He D.; Luo Y.; Shang W.; Jiang Y.; Liu M.; Zeng M.; Wang N., et al. Titanium Dioxide@Polyoxometalate-Organic Framework as an Efficient Photocatalyst for Dye Degradation under Visible Light Conditions. *Polyoxometalates*, **2025**, *4*, 9140089.

[143] Hu Q.; Chen S.; Wågberg T.; Zhou H.; Li S.; Li Y.; Tan Y.; Hu W.; Ding Y., et al. Developing Insoluble Polyoxometalate Clusters to Bridge Homogeneous and Heterogeneous Water Oxidation Photocatalysis. *Angew. Chem. Int. Ed.*, **2023**, *62*, 202303290.

[144] Díaz U.; Corma A. Ordered Covalent Organic Frameworks, COFs and PAFs. From Preparation to Application. *Coord. Chem. Rev.*, **2016**, *311*, 85-124.

Table of Contents

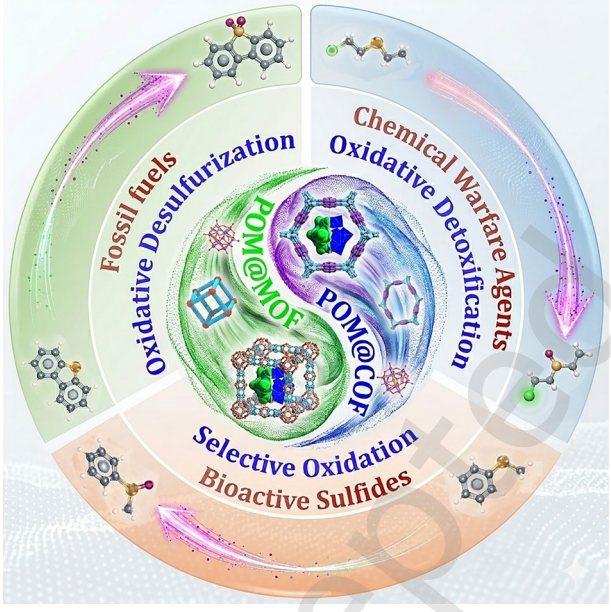

This review systematically summarizes the progress of synergistic catalysis in POM@MOF and POM@COF Composites in the fields of bioactive sulfide synthesis, fuel desulfurization and chemical warfare agent purification.

Author Abstract

Yanhong Chen received her B.S. degree in Chemistry from Henan University in 2017, M.S. degree in Inorganic Chemistry from Henan University under the guidance of Prof. Junwei Zhao in 2019, and Ph.D. degree in Inorganic Chemistry from Dalian University of Technology under the direction of Prof. Haiyan An in 2023. She is currently a lecturer at the School of Chemistry and Chemical Engineering, Hainan Normal University. Her current research mainly focuses on the synthesis and properties of Polyoxometalate-based complexes.

Shenzhen Chang was born in Henan, China in 1993. He received his B.S. degree in Chemistry from Henan University in 2016, and Ph.D. degree from Dalian University of Technology under the direction of Prof. Haiyan An in 2022 through a combined master-doctoral program. Then, he joined the School of Chemistry and Chemical Engineering, Hainan University. His research interests mainly focus on the molecular construction and application exploration of polyoxometalate-based functional materials.

Junwei Zhao received his B.S. degree in chemistry in 2002, his M.S. degree in 2005 from Henan University and his Ph.D. degree from the Fujian Institute of Research on the Structure of Matter, Chinese Academy of Sciences in 2008. After that, he joined the faculty of Henan University, was promoted to a full professor in chemistry in 2014, was appointed as a Distinguished professor of Henan Province in 2018, elected as a Fellow of the Royal Society of Chemistry in 2022 and recognized as a Zhongyuan Leading Talent in Fundamental Research in 2025. Currently, his research interests are mainly focused on the polyoxometalate-based functional materials and their optical, electric and biological properties and smart devices.